Kansas Geological Survey

Approximate analysis of saltwater mound development in an inland aquifer

by

Hillel Rubin
On leave from Department of Civil Engineering, Technion - Israel Institute of Technology, Haifa 32000, Israel

and

Robert W. Buddemeier
Kansas Geological survey, The University of Kansas, Lawrence, Kansas 66047, USA

Kansas Geological Survey Open File Report 98-34
September 1998

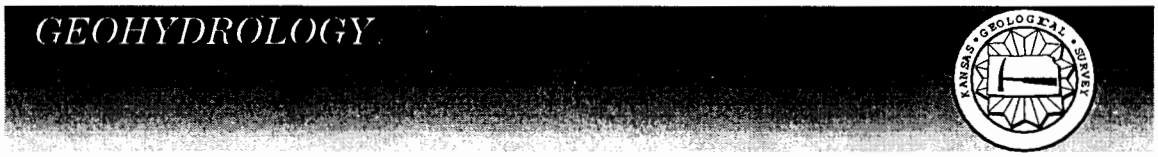

The University of Kansas, Lawrence, KS 66047 Tel.(785) 864-3965

Approximate analysis of saltwater mound development in an inland aquifer

Hillel Rubin[1] and Robert W. Buddemeier

Kansas Geological survey, The University of Kansas, Lawrence, Kansas 66047, USA

Abstract

This report concerns mineralization of groundwater resources in the Great Bend Prairie aquifer, south central Kansas, where saltwater originates from a deeper Permian bedrock formation. Based on field as well as theoretical studies it is assumed that the aquifer mineralization process occurs due to upward migration of salinity through various types of discontinuities in the impermeable layers separating the freshwater aquifer from the formation saturated with saltwater. A simplified conceptual model is adopted, in which the saltwater seeps into the aquifer through a discontinuity representing a semi-confining layer.

A top specified boundary layer (TSBL) approach is employed to describe and characterize the mineralization process. According to this approach various types of boundary layers (BLs) develop in the discontinuity region. They are termed bottom, inner, and outer BLs. It is predicted that in cases of high rates of saltwater seepage and low values of transverse dispersivity, a saltwater mound develops at the bottom of the aquifer. Downstream from the impermeable layer discontinuity the saltwater mound thickness decreases. The TSBL approach is also applied in this region to simulate changes of salinity distribution in the domain. Numerical simulations indicate that similar salinity profiles develop throughout the mineralized domain. Power coefficients typical of salinity distributions in the various BLs are determined, and calibration of the TSBL approach is achieved by comparison of the TSBL predictions to those provided by rigorous numerical simulations.

The study provides a set of definitions and terminology that are very convenient and helpful in visualizing the development of saltwater mounds in aquifers subject to mineralization. The TSBL approached is a simple and robust tool for initial characterization of the aquifer mineralization process. It can also be useful for the interpretation and evaluation of field monitoring results.

---

[1]On leave from Department of Civil Engineering, Technion - Israel Institute of Technology, Haifa 32000, Israel

Introduction

In several previous studies *(Rubin and Buddemeier, 1996, 1998a; b; c; d)* the authors have analyzed various characteristics of inland aquifer mineralization processes. Those studies, as well as the present study, originate from interest in the degradation of groundwater quality in the Great Bend Prairie aquifer, south central Kansas.

Garneau (1995) provided a comprehensive survey of previous studies aimed at the identification of the geological formations and stratigraphy of the Great Bend Prairie aquifer. In the following paragraphs we provide a brief overview of this topic.

Layton and Berry (1973) and Fader and Stullken (1978) describe the geohydrology of the Quaternary Great Bend Prairie aquifer. The aquifer is an alluvial aquifer composed of unconsolidated fluvial, lacustrine and eolian deposits of gravel, sand, silt and clay. Gravel and coarse sand deposits represent stream channel and bar lateral accretion surfaces *(Collinson, 1986).* Fluvial deposits of fine sand, silt and clay occur between the channels as levee, crevasse splay and overbank flood deposits *(Collinson, 1986).* Fine-grained sediments can also accumulate as abandoned channel plugs and thus form thick, lens-shaped bodies of limited lateral extent.

Lacustrine deposits of fine-grained sediments form lens-shaped bodies of great lateral extent compared to thickness *(Allen and Collinson, 1986).*

Fine-grained dune sand and loess (*Welch and Hale, 1987*) typically represent eolian deposits. Dune sand, from sources along the Arkansas River, and loess deposits currently form a veneer over much of the Great Bend Prairie *(Fader and Stullken, 1978).* Three other major loess deposits are described in central Kansas representing the Loveland, Poeria and Bignell formations *(Bayne and O'Connor, 1968).* Thickness values of the usually sheet-like loess deposits in south-central Kansas are uncertain and can be expected to be highly variable as aresult of reworking by erosion *(Welch and Hale, 1987).* Minor air-fall and rework deposits of volcanic ashes have been detected in the alluvium with possible sources from eruptions in California, Wyoming and New Mexico *(Ward et al., 1993; Boellstorff, 1976).*

Extensive clay layers have also developed in the Great Bend Prairie aquifer as the product of soil formation. Paleosols of Quaternary age in central Kansas include the

Afton, Yarmouth, Sangamon and Brady soils *(Bayne and O'Connor, 1968).* Caliche horizons, usually associated with soil formation *(Allen, 1974),* are included on several well driller's lithologic logs and indicate the presence of paleosols *(Stullken and Fader, 1976; Buddemeier et al., 1993; Gillespie and Hargadine, 1994).* Thickness of clay layers developed from soil formation depend on the climate, length of time of soil development and the nature of the parent material *(Collinson, 1986).* With regard to loess deposits, information on paleosol thickness and extent within the Great Bend Prairie aquifer is vague and incomplete.

Generally, it is well established that saltwater intrudes into the Great Bend Prairie aquifer where the shallow aquifer is in contact with the underlying Permian bedrock formations. The latter contains evaporites such as halite and anhydrite. However, the configuration and distribution of clay layers within the Great Bend Prairie aquifer are important factors to consider since these low-permeability horizons can control the vertical movement and distribution of solutes in the groundwater. Saltwater, seeping from the bedrock, can be effectively confined below an extensive clay layer. Alternating sand and clay layers can also influence the vertical and lateral advection and macrodispersion of solute within the aquifer.

Field measurements *(Buddemeier et al., 1994; Garneau 1995, Young and Rubin, 1998),* as well as theoretical studies *(Rubin and Buddemeier, 1998b, d)* have indicated that in many places the aquifer mineralization originates from seepage of saltwater through discontinuities in clay lenses and layers which act as semi-confining layers. *Rubin and Buddemeier (1998b; d)* have investigated this type of groundwater mineralization and show that the top specified boundary layer (TSBL) method *(Rubin and Buddemeier, 1996)* can be applied to the calculation, quantification and analysis of the mineralization outcomes. However, results suggest that, in cases of comparatively high rates of saltwater seepage and small values of the dispersivity, saltwater mounds develop in the mineralized aquifer. The present study applies the TSBL method to calculation of the development of such mounds.

The conceptual model and basic formulation

We refer to the simplified conceptual model shown in Fig. 1, which depicts a local semi-confining discontinuity in an impermeable layer separating saline bedrock from the overlying freshwater alluvial aquifer. This discontinuity allows seepage of saltwater from the comparatively high-head region in the deep formation into the lower head region of the freshwater aquifer. The length of the discontinuity is x_e^*. We adopt a Cartesian coordinate system whose x^* axis represents the horizontal longitudinal direction, and the y^* axis represents the vertical direction. The coordinate system origin is located at the upstream side of the impermeable layer discontinuity.

Flow conditions and salinity transport in the complete domain of Fig. 1 are governed by the following set of differential equations

$$\vec{q} = -\frac{k}{\mu}(\nabla p - \rho \vec{g}) \tag{1}$$

$$\frac{\partial C^*}{\partial t^*} + \vec{V} \cdot \nabla C^* = \nabla \cdot (\tilde{D} \cdot \nabla C^*) \tag{2}$$

where $\vec{q}$ is the specific discharge vector, k is the permeability, μ is the fluid viscosity, p is the pressure, ρ is the fluid density, g is the gravitational acceleration, C^* is the salt concentration (salinity), V is the interstitial flow velocity, D is the dispersion tensor, t^* is time.

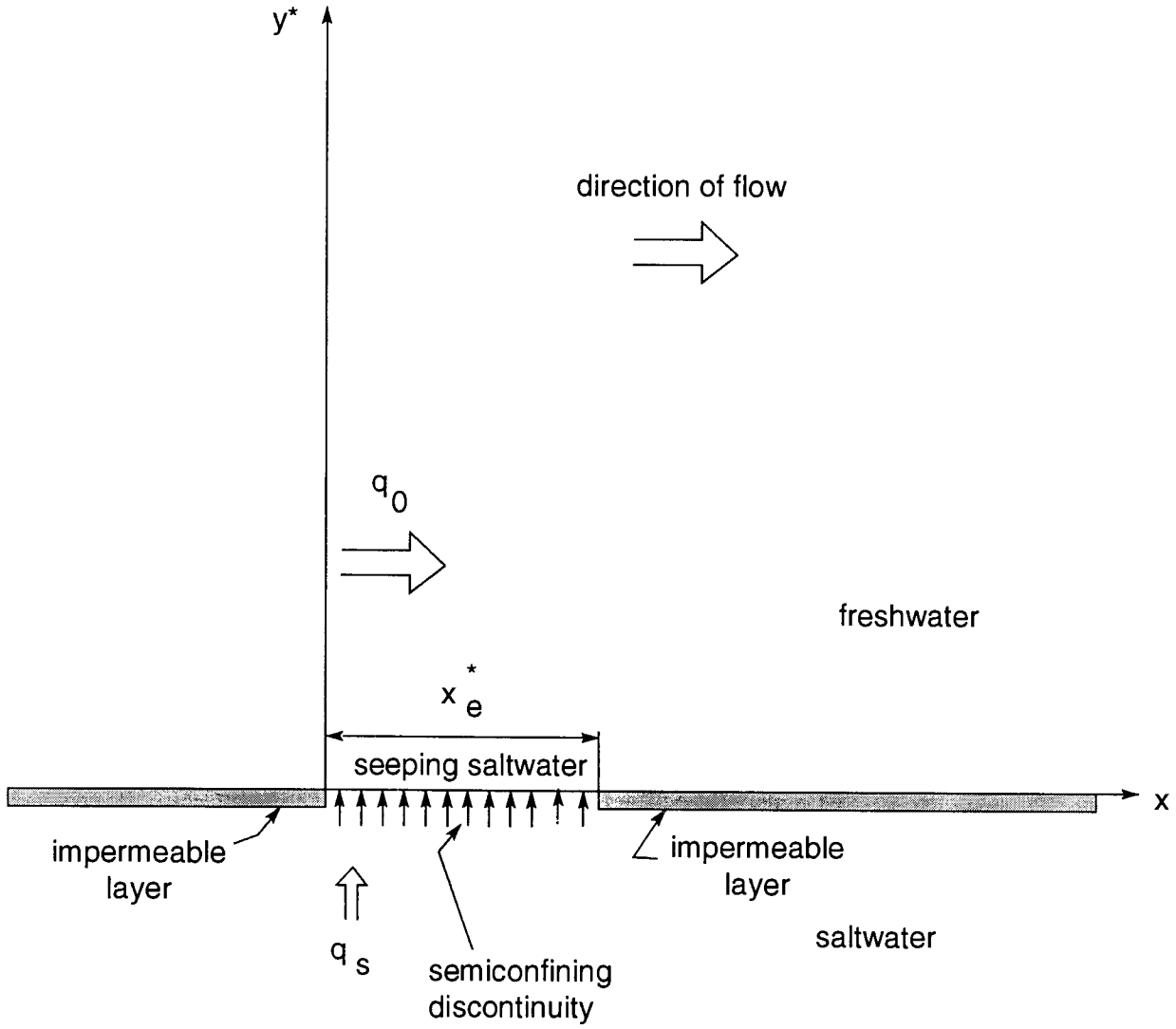

Figure 1 Schematic description of the simulated domain and coordinate system

Equations (1) and (2) can be solved by various types of numerical procedures (e.g. *Reeves et al., 1986)*. However, the simultaneous solution of eqs. (1) and (2) is quite complicated; the non-linearity stemming from the dependence of ρ on C^* introduces simulation difficulties, and there are problems of stability of the numerical solution, numerical dispersion, etc. Therefore, simplification into the calculation of salinity transport in the domain of Fig. 1 is very desirable. Such simplification should be consistent with an overall methodology of groundwater quality simulation and should proceed in stages. The initial stage of such a methodology consists of general quantitative evaluation of phenomena and of time scales of contamination and reclamation, as well as initial risk analysis. The present paper addresses such a limited initial stage. Possible simplifications of eqs. (1) and (2) for the initial stage of groundwater quality calculation in the domain of Fig. 1 are given in following paragraphs.

Initially, the upper part of the domain, represented by $y \geq 0$, is occupied by freshwater, and there is no flow through the semi-confining discontinuity in the impermeable layer, whose length is x_e^*. Initially the salinity is zero in the region given by

$$y^* = 0, \quad 0 \leq x^* \leq x_e \tag{3}$$

We ignore effects of salinity on the groundwater viscosity. We also employ the Dupuit approximation and consider that streamlines are horizontal. Then eq. (1) indicates that the velocity V is uniformly distributed in the domain, and has only a component in the x^* direction. Therefore, salinity transport in the domain is governed by

$$\frac{\partial C^*}{\partial t^*} + V\frac{\partial C^*}{\partial x^*} = D_x\frac{\partial^2 C^*}{\partial x^{*2}} + D_y\frac{\partial^2 C^*}{\partial y^{*2}} \tag{4}$$

where x^* and y^* are the longitudinal and vertical coordinates, respectively, and D_x and D_y are the longitudinal and transverse dispersion coefficients, respectively.

In a previous study *(Rubin and Buddemeier, 1998d)* the authors demonstrated by numerical simulations that it is appropriate to use eq. (4) for estimation of the development of various boundary layers (BLs) in the region of the impermeable layer discontinuity.

The uniformity of the physical parameters in the domain of Fig. 2 invites the replacement of the physical coordinates and variables with dimensionless quantities, defined by

$$x = \frac{x^*}{l_0}; \quad y = \frac{y^*}{l_0}; \quad t = \frac{t^* V}{l_0}; \quad C = \frac{C^* - C_f^*}{C_s^* - C_f^*} \tag{5}$$

where l_0 is an adopted unit length, and C_f^* and C_s^* are salinity values of the fresh and saltwater, respectively.

Introducing the dimensionless variables of eq. (5) into eq. (4), we obtain

$$\frac{\partial C}{\partial t} + \frac{\partial C}{\partial x} = a_L \frac{\partial^2 C}{\partial x^2} + a \frac{\partial^2 C}{\partial y^2} \tag{6}$$

where a_L and a are the dimensionless longitudinal and transverse dispersivities, respectively. These variables are defined by

$$a_L = D_x / (l_0 V); a = D_y / (l_0 V) \tag{7}$$

The conceptual model shown in Fig. 1 refers to saltwater seepage through the impermeable layer discontinuities. The appropriate set of initial and boundary conditions relevant to this case is

$$C = C(x, y, t), \; x, y, t \geq 0 \tag{8}$$

$$C(x, y, 0) = 0 \tag{9}$$

$$C(x, \infty, t) = 0 \tag{10}$$

$$\frac{\partial C}{\partial x} \to 0 \quad at \quad x \to \infty \tag{11}$$

$$-a \frac{\partial C}{\partial y} = q_R (1 - C) \quad at \quad y = 0, 0 \leq x \leq x_e \tag{12}$$

$$\frac{\partial C}{\partial y} = 0 \quad at \quad y = 0, x_e \leq x \leq \infty \tag{13}$$

where x_e is the dimensionless length of the impermeable layer discontinuity.

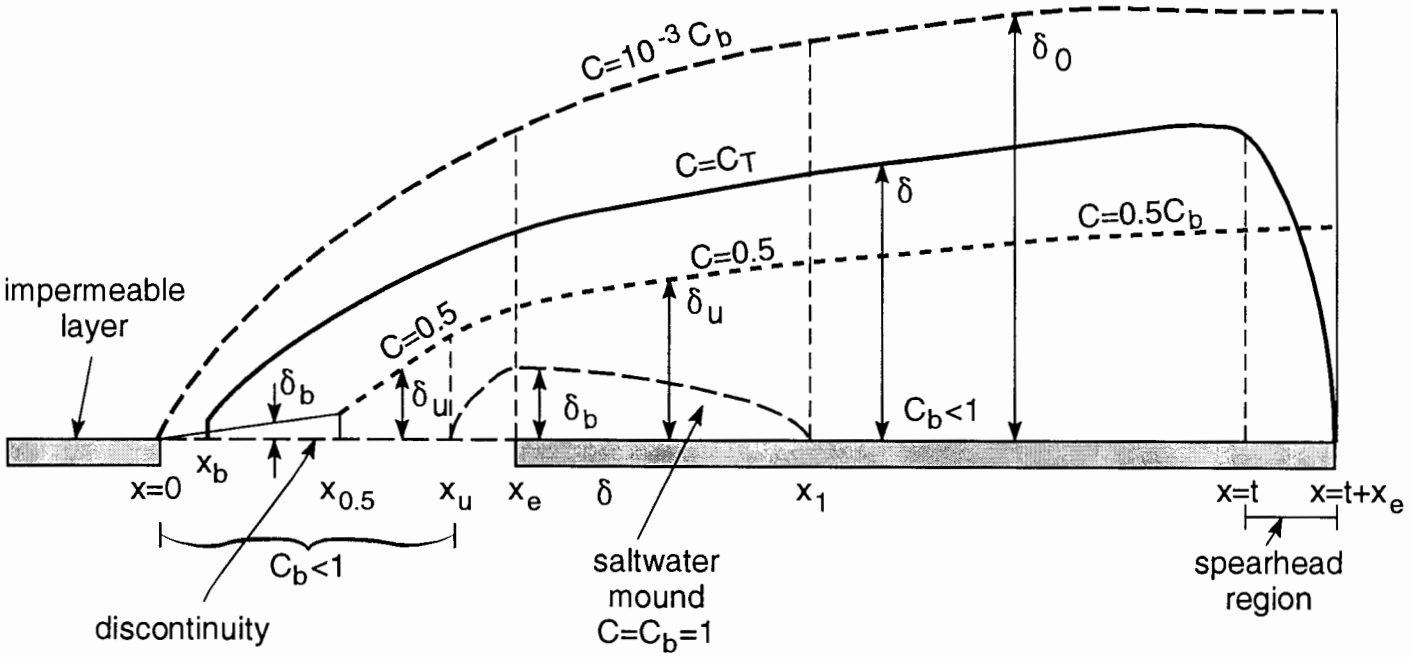

Figure 2 The saltwater mound and the various types of BLs developed in the simulated domain, with the terms and symbols (see Notation) used

Numerous simulations of contaminant penetration through the free surface of aquifers *(Rubin and Buddemeier, 1996)* have been performed. Such simulations, as well as simulations of salinity intrusion into an inland aquifer through its bottom *(Rubin and Buddemeier, 1998a; b; c; d)*, have indicated that salinity transport can be well represented while ignoring the first right hand side term of eq. (6). If this term is neglected then the boundary condition given by eq. (11) is not needed.

The boundary condition given by eq. (12) requires specification of vertical flow velocities. However, we can ignore the vertical flow velocities and keep the essence of this boundary condition by dividing x-values into the following ranges

$$0 \le x \le x_{0.5} \tag{14}$$

$$x_{0.5} \le x \le x_u \tag{15}$$

$$x_u \le x \le x_e \tag{16}$$

$$x_e \le x \le x_1 \tag{17}$$

$$x_1 \le x \le \infty \tag{18}$$

where $x_{0.5}$ is the x-value at which the salinity at the bottom boundary becomes 0.5, and x_u is the x-value at which the salinity at the bottom boundary reaches unity. At this point the saltwater mound starts to develop. The x-value downstream of x_e at which the salinity at the bottom boundary diminishes below unity is x_1. At this point the saltwater mound vanishes. In a previous study *(Rubin and Buddemeier, 1998d)* the authors referred to cases in which the saltwater mound does not develop (i.e. cases of comparatively small values of q_R/a). Therefore, there was no reference in that study to values of x_u and x_1. In the following paragraphs we provide a description of the various types of BLs developed in each range of x-values given by eqs. (14) - (18). A brief review of the various formulations is given whenever the results of *Rubin and Buddemeier (1998d)* could be applied. Complete analysis and development of basic formulations are given for ranges of x-values which have not been covered by the previous study (*Rubin and Buddemeier 1998d).* Ranges of the different x-values and the definitions of the various BLs are shown

in Fig. 2. Figure 3 shows the various mass fluxes through the BLs developed in each range of x-values.

It should be noted that in the BL method, some specific power laws represent approximate relationships between normalized coordinates and the normalized salinity profile for each range of x-values. Compliance with the conservation of mass requires that at each interface between adjacent ranges of x-values some adjustment would be made with regard to quantities characterizing the BL development. Appendix E provides details about the BL adjustment at each interface in the domain of Fig. 2.

Range of x-values $0 \leq x \leq x_{0.5}$

In this range of x-values the domain is divided into two regions as shown in Fig. 2. At the bottom of the originally freshwater aquifer we assume that a region of almost uniform salinity distribution is subject to build-up at $0 \leq y \leq \delta_b$. This region is termed the bottom BL. The value of the salinity there is C_b. On top of the bottom BL, the outer BL develops. In this region the salinity varies between C_b and $10^{-3}C_b$. At the top of the outer BL the salinity practically vanishes, (i.e. it is smaller than some acceptable value, C_T, by at least an order of magnitude). For the purpose of this study, we take $C_T = 0.01$. At $x = x_{0.5}$ the value of C_b is 0.5. Basic analytical presentation of the bottom and outer BLs has been made in a previous study *(Rubin and Buddemeier, 1998d)*. Only a brief review of that presentation is given in Appendix A of this report. In following paragraphs, the essences of the analysis and calculation results are presented

Whereas, in the bottom BL salinity is uniformly distributed, we assume that in the outer BL the salinity profile is given by:

$$C = C_b(1-\eta)^n; \quad \eta = \frac{y-\delta_b}{\delta_0-\delta_b} \tag{19}$$

From this assumption and the BL treatment of salinity transport in the domain, as shown in Appendix A, we obtain expressions for the determination of C_b, x, δ_b and δ, respectively:

$$C_b = \frac{\tau}{\tau + an/q_R} \tag{20}$$

where τ is a modified coordinate, equal to the difference between the outer and bottom BLs.

$$x = \frac{H(\tau)}{an(n+1)} \tag{21}$$

where

$$H(\tau) = \frac{1}{2}\tau^2 + \frac{an}{q_R}\tau - \left(\frac{an}{q_R}\right)^2 \ln\left(1 + \tau\frac{q_R}{an}\right) \tag{22}$$

$$C_b\delta_b = \frac{q_R}{an(n+1)}\left[\frac{1}{2}\tau^2 + \left(\frac{an}{q_R}\right)^2 - \left(\frac{an}{q_R}\right)^3\left(\frac{1}{\tau + an/q_R}\right) - \left(\frac{an}{q_R}\right)^2 \ln\left(1 + \tau\frac{q_R}{an}\right)\right] \tag{23}$$

$$\delta = \delta_b + \tau - \tau^{1-1/n}\left[C_T(\tau + an/q_R)\right]^{1/n} \tag{24}$$

The set of eqs. (19) – (24) completely describes the salinity profile buildup in the range of x-values $0 \le x \le x_{0.5}$. Equation (21) refers to the steady state condition, at which the buildup of the bottom BL is completed. It should be noted that eq. (24) is applicable only if $C_b \ge C_T$. At the upstream portion of the discontinuity the value of C_b is smaller than C_T. At that location the region of interest (ROI), which is a top specified BL (TSBL) does not develop.

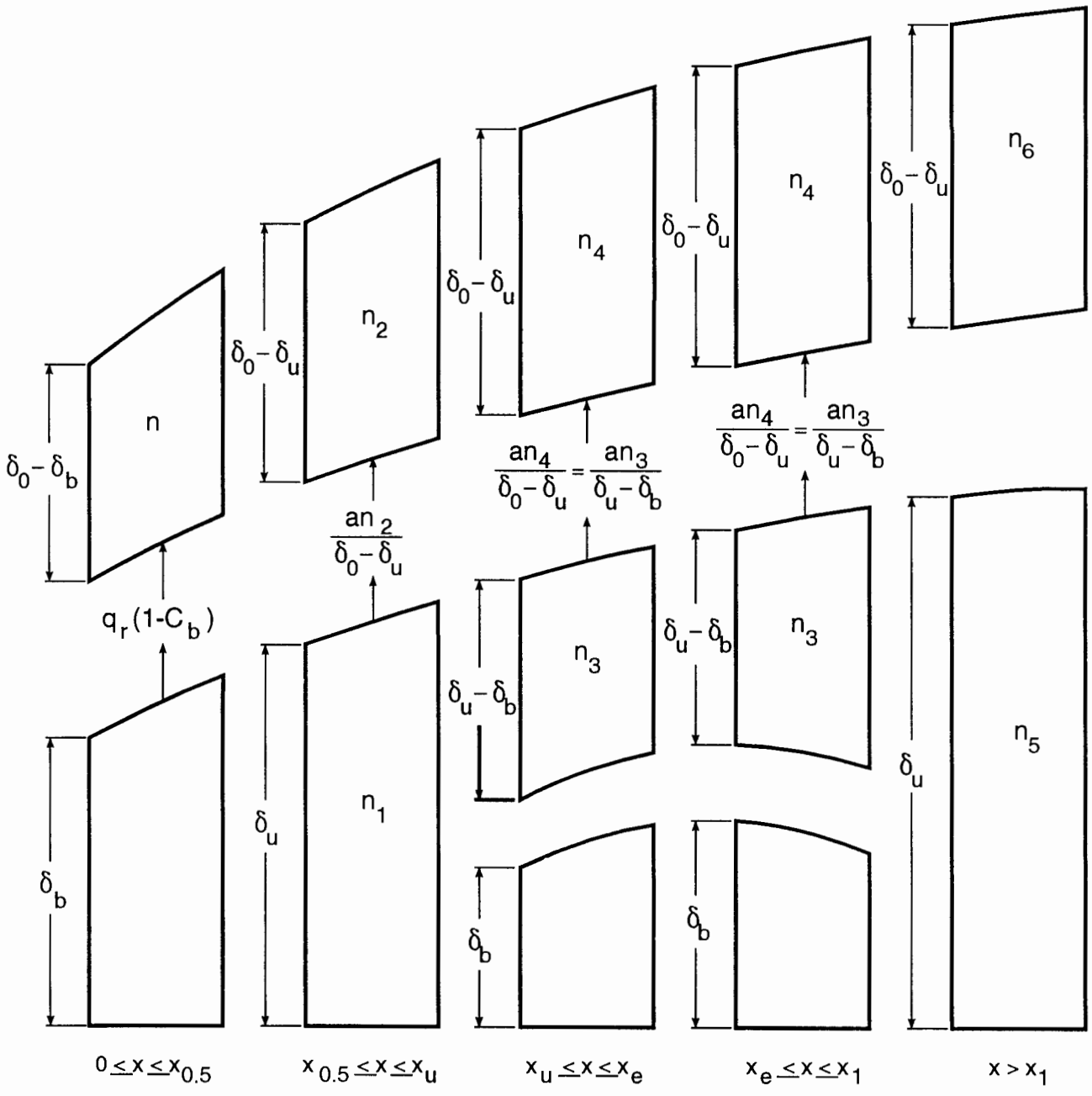

Figure 3 Fluxes of salinity between the various BLs and power coefficients typical of the various BLs

Range of x-values $x_{0.5} \le x \le x_u$

In this range of x-values we divide the domain into two regions as shown in Figs. 2 and 3. At the bottom of the originally freshwater aquifer we consider that an inner BL is built-up at $0 \le y \le \delta_u$. The salinity in this region varies between $C = C_b$ and $C = 0.5$. On top of the inner BL, the outer BL develops at $\delta_u \le y \le \delta_0$. The salinity in the outer BL varies between $C = 0.5$ and a negligible value, which is defined as salinity smaller than C_T by at least an order of magnitude.

Basic analytical presentation of the inner and outer BLs has been made in a previous study *(Rubin and Buddemeier, 1998d)*. Only a brief review of that presentation is given in Appendix B of this report.

As shown in Appendix B, the inner BL incorporates the following salinity profile

$$C = C_b - (C_b - 0.5)(1-\xi)^{n_1}; \quad \xi = \frac{\delta_u - y}{\delta_u}; \quad 0 \le y \le \delta_u \tag{25}$$

The outer BL incorporates the following salinity profile

$$C = 0.5(1-\eta)^{n_2}; \quad \eta = \frac{y - \delta_u}{\delta_0 - \delta_u}; \quad \delta_u \le y \le \delta_0 \tag{26}$$

The expressions for the development of the inner and outer BLs are given, respectively by:

$$(\delta_0 - \delta_u)^2 = 2n_2(n_2+1)(x - x_{0.5}) + (\delta_0 - \delta_b)_{x=x_{0.5}} \tag{27}$$

$$\delta_u = \frac{(n_1+1)(\delta_0 - \delta_u)}{2n_2}\left[(1+F)^{0.5} - 1\right] \tag{28}$$

where

$$F = \frac{8fn_2}{(n_1+1)(\delta_0 - \delta_u)} \tag{29}$$

$$f = q_R(x - x_{0.5}) - \frac{\delta_0 - \delta_u}{2(n_2+1)} + \left[\frac{\delta_0 - \delta_b}{2(n_2+1)} + \frac{\delta_b}{2}\right]_{x=x_{0.5}} \tag{30}$$

The top of the ROI is again defined by the isohaline $C = C_T$. Equation (26) yields

$$\eta_T = 1 - (2C_T)^{1/n_2} \tag{31}$$

$$\delta = \delta_u + (\delta_0 - \delta_u)\eta_T \tag{32}$$

The salinity value at the bottom of the aquifer is given by

$$C_b = 0.5\left[1 + \frac{n_2}{n_1}\frac{\delta_u}{\delta_0 - \delta_u}\right] \tag{33}$$

Range of x-values $x_u \le x \le x_e$

As shown by Figs. 2 and 3, in this range of x-values, we divide the domain into the bottom BL with thickness δ_b, the inner BL, whose top is located at $y = \delta_u$, and the outer BL with top at $y = \delta_0$. The bottom BL incorporates completely saline water, and represents the saltwater mound buildup in the freshwater aquifer. Salinity distributions in the bottom, inner and outer BLs are given, respectively by:

$$C = C_b = 1 \quad at \quad 0 \le y \le \delta_b \tag{34}$$

$$C = 1 - 0.5(1 - \xi)^{n_3}; \quad \xi = \frac{\delta_u - y}{\delta_u - \delta_b} \quad at \quad \delta_b \le y \le \delta_u \tag{35}$$

$$C = 0.5(1 - \eta)^{n_4}; \quad \eta = \frac{y - \delta_u}{\delta_0 - \delta_u} \quad at \quad \delta_u \le y \le \delta_0 \tag{36}$$

Appendix C provides the complete analysis and calculation of the BL development in this range of x-values. It is shown that the various BL thickness values are:

$$\delta_b = \alpha_3 q_R (x - x_u) - \frac{1}{2(n_4+1)}\left[(\delta_0 - \delta_u) - (\delta_0 - \delta_u)_{x=x_u}\right]$$

$$-\frac{n_3+0.5}{n_3+1}\left[(\delta_u - \delta_b) - (\delta_u)_{x=x_u}\right] \quad (37)$$

$$(\delta_u - \delta_b)^2 = \alpha_1 a \frac{n_3(n_3+1)}{n_3+0.5}(x - x_u) + (\delta_u^2)_{x=x_u} \quad (38)$$

$$(\delta_0 - \delta_u)^2 = 2\alpha_2 a n_4 (n_4+1)(x - x_u) + (\delta_0 - \delta_u)^2_{x=x_u} \quad (39)$$

where α_i (i = 1, 2,3) are coefficients, which should be determined by best fit of the model to numerical simulations or field data.

With regard to the determination of the ROI, it should be noted that eqs (31) and (32) are also applicable to this range of x-values.

Range of x-values $x_e \leq x \leq x_1$

In this region all expressions represented in the preceding range of x-values are applicable, except for eq. (37) whose first right hand side term vanishes, as there is no seepage of saltwater into the domain. Without this term, due to the development and expansion of δ_0 and δ_u, the value of δ_b should decrease. Therefore in this range of x-values, the thickness of the saltwater mound decreases. By adapting eq. (37), we obtain the following expression for the thickness of the saline bottom BL, which represents the thickness of the saltwater mound.

$$\delta_b = (\delta_b)_{x=x_e} - \frac{\alpha_4}{2(n_4+1)}\left[(\delta_0 - \delta_u) - (\delta_0 - \delta_u)_{x=x_e}\right]$$

$$-\alpha_4 \frac{n_3+0.5}{n_3+1}\left[(\delta_u - \delta_b) - (\delta_u - \delta_b)_{x=x_e}\right] \quad (40)$$

where α_4 is a calibration coefficient.

Expressions for other BLs given by eqs.(38) and (39) are also applicable in this range of x-values.

Range of x-values $x \geq x_1$

Downstream of x_1, Figs. 2 and 3 show that the domain incorporates inner and outer BLs. There is no salinity transfer between these two BLs, as indicated by Fig. 3; vertical salinity gradients only lead to expansion of the BLs. This figure also the various power coefficients associated with the salinity distributions in the domain.

The salinity distribution in the inner BL is given by

$$C = C_b[1-(1-c_r)(1-\xi)^{n_5}]; \quad \xi = \frac{\delta_u - y}{\delta_u}; \quad 0 \leq y \leq \delta_u \tag{41}$$

where c_r is the ratio between the salinity at $y=\delta_u$ and the salinity C_b occurring at $y = 0$.

The salinity profile in the outer BL is given by

$$C = c_r C_b(1-\eta)^{n_6}; \quad \eta = \frac{y-\delta_u}{\delta_0 - \delta_u}; \quad \delta_u \leq y \leq \delta_0 \tag{42}$$

Appendix D provides a brief description of the complete analysis and calculations referring to this range of x-values. The analysis and calculations are very similar to those of *Rubin and Buddemeier (1998c)*. Minor differences between the calculations of that study and the present one originate from the presence of the saltwater mound. According to numerical simulations of *Rubin and Buddemeier (1998c)* the best fit values of power laws of eqs. (41) and (42) are:

$$n_5 = 1.84 \quad \text{and} \quad n_6 = 4. \tag{43}$$

At $t=x_1+x_e$ the salinity distribution at $x = x_1$ is subject to steady state conditions, as implied by calculations for $x \leq x_1$. At $x \geq t+x_e$ there is no salinity penetration. Between $x = x_1$ and $x = t+x_e$ values of the inner and outer BL thickness are given by

$$(\delta_u^2)_{x,t} = (\delta_u^2)_{x=x_1,t_1=t-x+x_1} + \frac{\alpha_5 a(1-c_r)n_5(n_5+1)}{n_5+c_r}(x-x_1) \tag{44}$$

$$(\delta_0-\delta_u)^2_{x,t} = (\delta_0-\delta_u)_{x=x_1,t_1=t-x+x_1} + 2\alpha_6 a n_6(n_6+1)(x-x_1) \tag{45}$$

where α_5 and α_6 are calibration coefficients. *Rubin and Buddemeier (1998c, d)* found that:

$$\alpha_5 = 0.935 \quad \text{and} \quad \alpha_6 = 0.775 \tag{46}$$

As there is no salinity transfer between the inner and outer BLs, we obtain

$$(C_b)_x = (\delta_u C_b)_{x_1} / (\delta_u)_x \tag{47}$$

The ROI is again defined as the region in which the salinity exceeds its acceptable value, C_T. Therefore, ROI is represented as a top specified boundary layer (TSBL) whose thickness is δ.

If $\delta_u < \delta < \delta_0$ then

$$\eta_T = 1-\left(\frac{C_T}{c_r C_b}\right)^{1/n_6};\ \delta = \eta_T\delta_0 + (1-\eta_T)\delta_u \tag{48}$$

If $0 < \delta < \delta_u$ then

$$\xi_T = 1-\left(\frac{1-c_r/C_b}{1-c_r}\right)^{1/n_5};\ \delta = \delta_u(1-\xi_T) \tag{49}$$

where ξ_T is the value of ξ at $y=\delta$.

The analysis and calculations imply that the horizontal penetration of the salinity creates two regions of horizontal salinity penetration, as shown in Fig. 2. The first is termed the "steady state region", and the second is termed the "spearhead region". The length of the spearhead region is constant, and it is equal to x_e. The steady state region is extended during the process of salinity penetration into the aquifer in the horizontal direction.

Preliminary tests

Our major objective in this study is to characterize the development of the saltwater mound region. Therefore our tests mainly address the range of x-values given by $x_u \leq x \leq x_1$. Other ranges of x-values have basically been characterized in a previous report *(Rubin and Buddemeier, 1998d)*. However, as shown hereafter some of these previous tests should also apply to $x > x_1$.

In our preliminary numerical experiments we consider that the saltwater mound comprises the region in which $0.99 \leq C \leq 1.0$. Therefore, by numerical solution of eqs.(1) and (2), which are very close to the approximate solutions of these differential equations *(Rubin and Buddemeier, 1998d),* we can identify the best fit values for the power coefficients n_3 and n_4. Other power coefficients have already been determined by *Rubin and Buddemeier (1998d)*. However, we also check possible effects of the saltwater mound on power coefficients characterizing the range $x > x_1$.

Figure 4 shows some examples of the development of the saltwater mound and the various types of BL, as implied by the numerical solution of eqs.(1) and (2). In Fig. 4 we identify the various BLs according to criteria which vary with the ranges of x-values as specified in the following expressions.

Range of x-values $0 \leq x \leq x_b$

In this range of x-values $C_b < 0.01$ and definitions of the various BLs are

$$\delta_b,\ \delta_u,\ \delta = 0; \quad \delta_0 = y \quad at \quad C = 0.001\ C_b \tag{50}$$

Range of x-values $x_b \leq x \leq x_{0.5}$

In this range of x-values $0.01 \leq C_b \leq 0.5$ and definitions of the various BLs are:

$$\delta_b = \delta_u = y \quad where \quad C = 0.99 C_b; \quad \delta = y \quad where \quad C = 0.01;$$

$$\delta_0 = y \quad where \quad C = 0.001 C_b \tag{52}$$

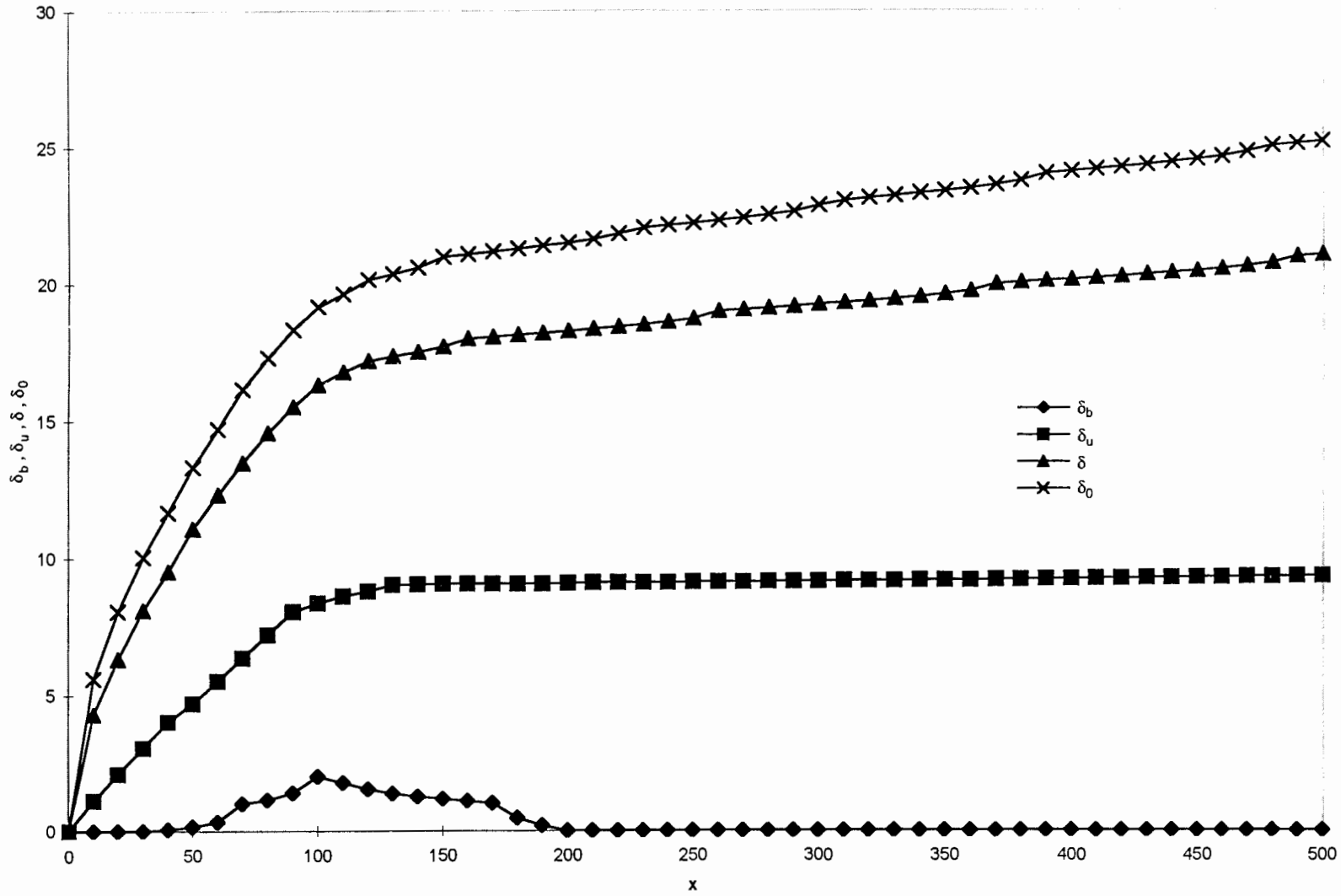

Figure 4a Numerical simulation results describing the development of the saltwater mound and the various BLs ($q_R = 0.1$, $x_e = 100$). See Fig. 2.

(a) $a = 0.02$; $x_{max} = 500$

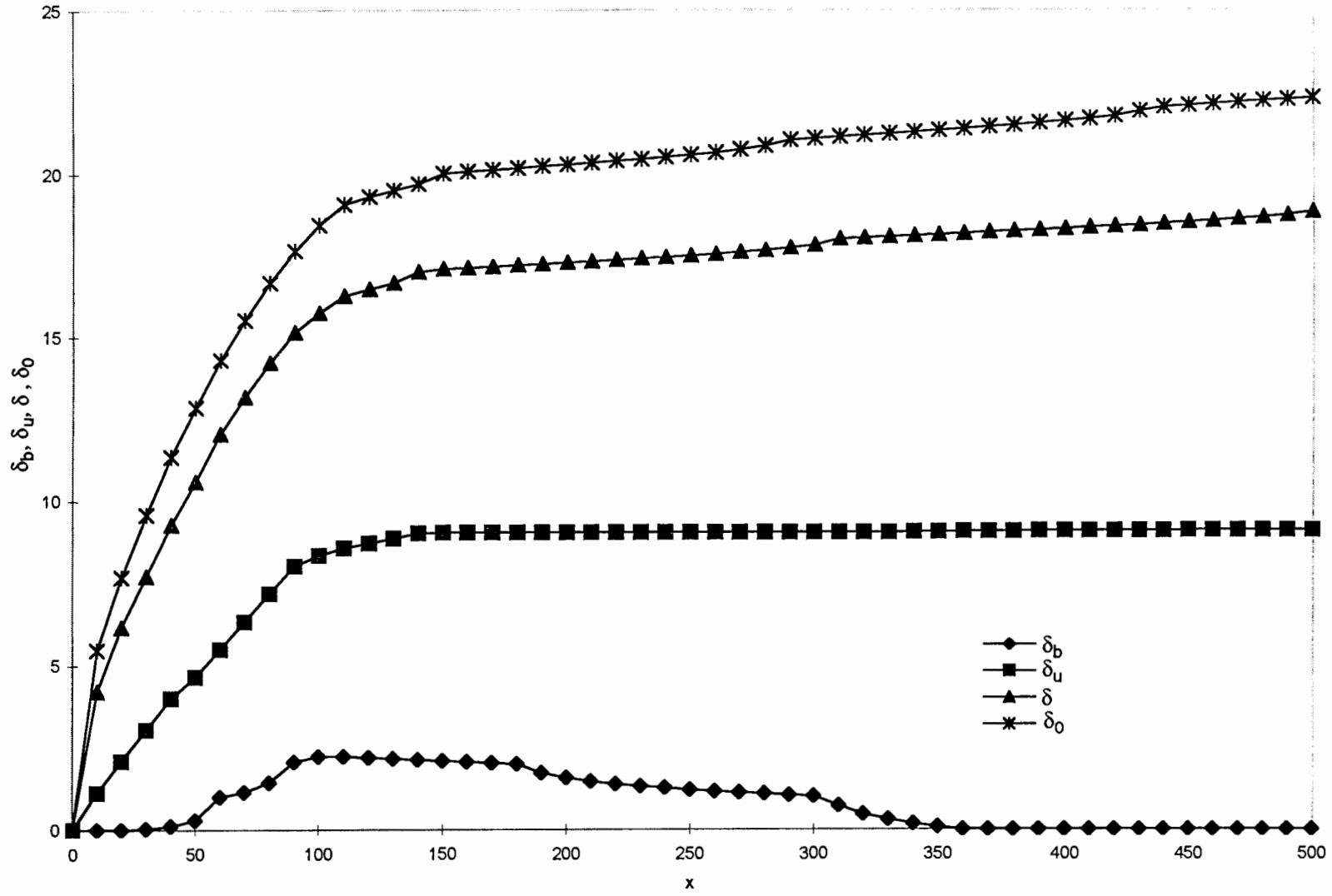

Figure 4b Numerical simulation results describing the development of the saltwater mound and the various BLs ($q_R = 0.1$, $x_e = 100$). See Fig. 2.

(b) $a = 0.01$; $x_{max} = 500$

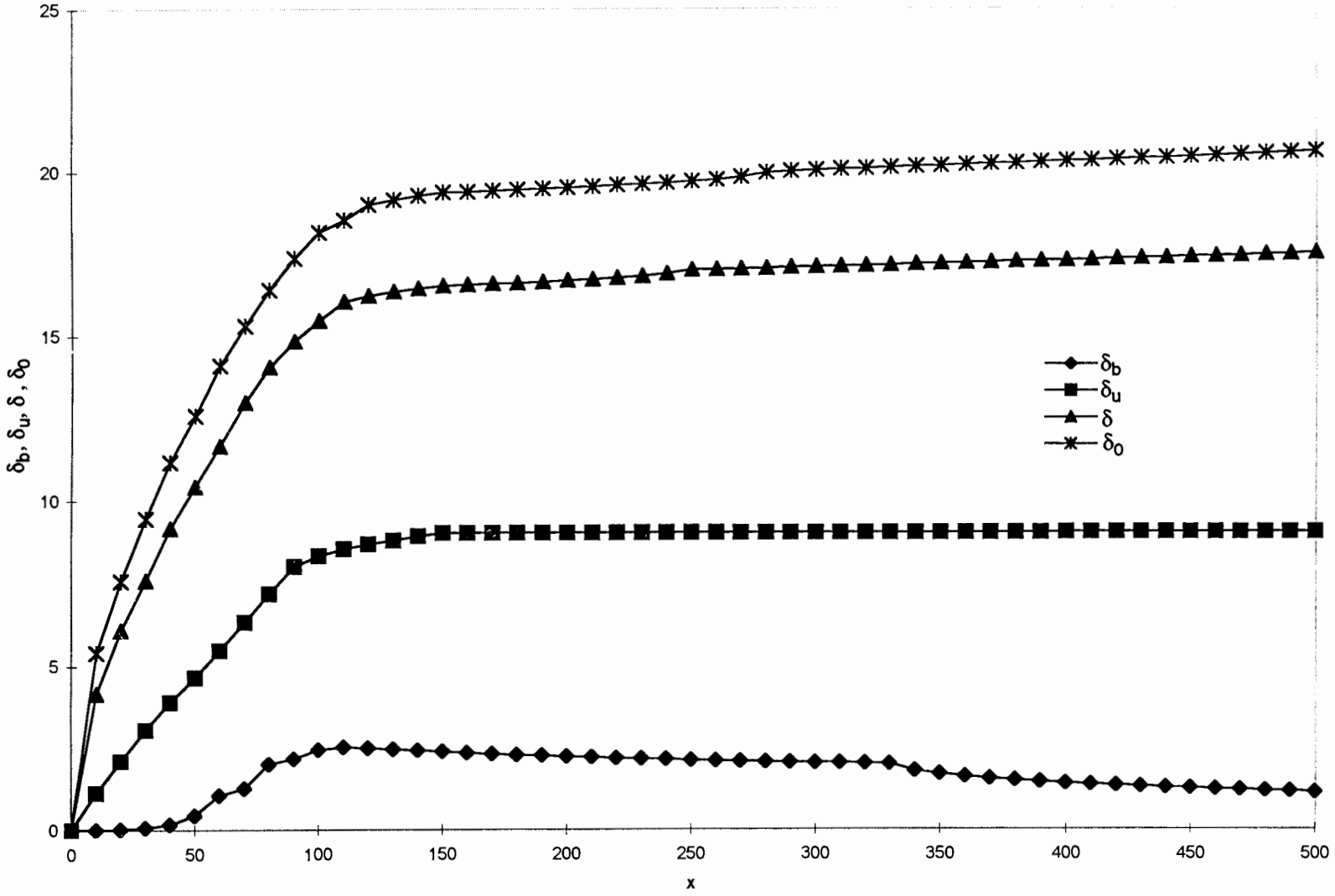

Figure 4c Numerical simulation results describing the development of the saltwater mound and the various BLs ($q_R = 0.1$, $x_e = 100$). See Fig. 2.

(c) $a = 0.005$; $x_{max} = 500$

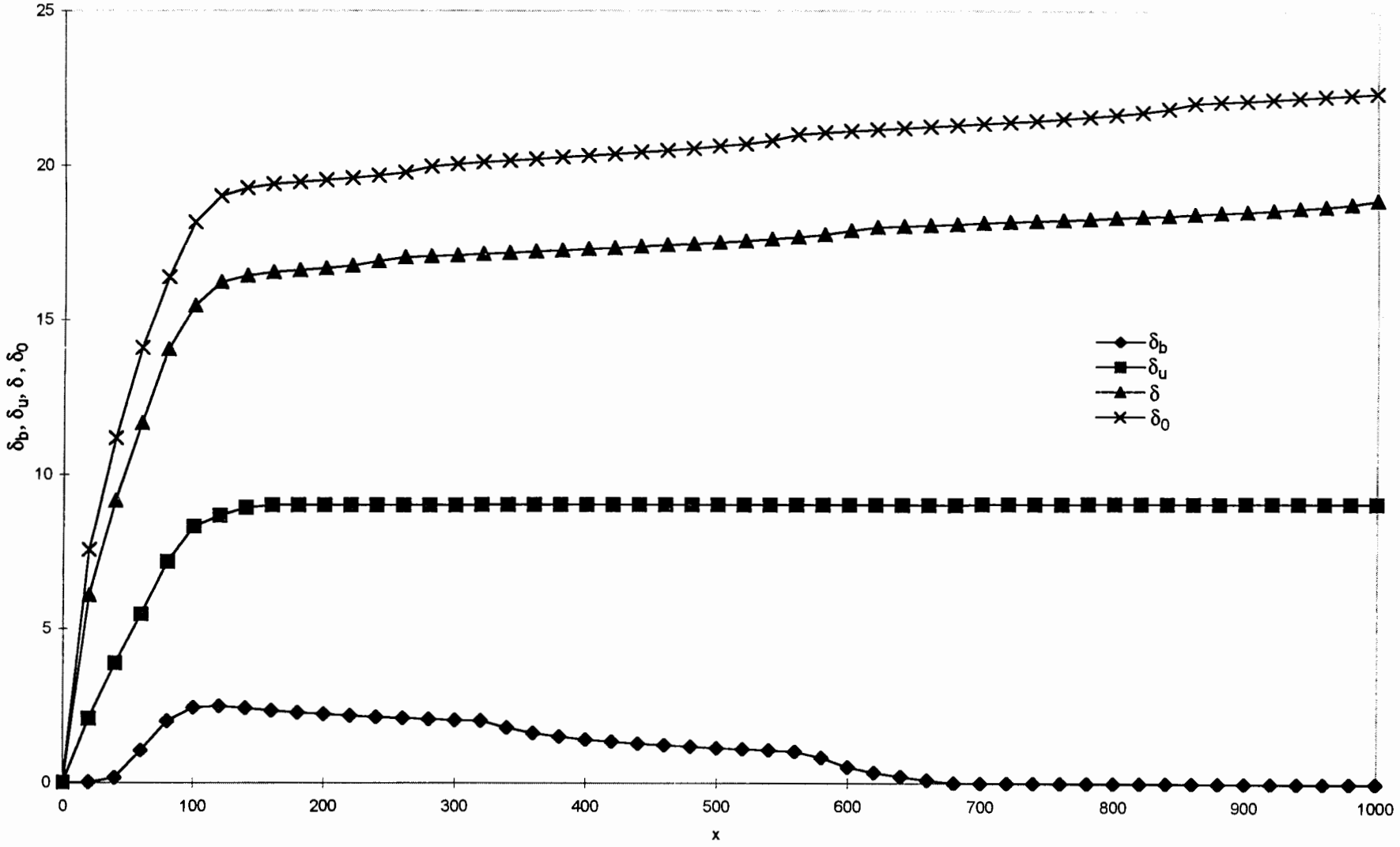

Figure 4d Numerical simulation results describing the development of the saltwater mound and the various BLs ($q_R = 0.1$, $x_e = 100$). See Fig. 2.

(d) $a = 0.005$; $x_{max} = 1000$

Range of x-values $x_{0.5} \leq x \leq x_u$

In this range of x-values $0.5 \leq C_b \leq 0.99$ and the definitions of the various BLs are:

$$\delta_b = 0; \quad \delta_u = y \quad where \quad C = 0.5; \quad \delta = y \quad where \quad C = 0.01;$$

$$\delta_0 = y \quad where \quad C = 0.001C_b \tag{53}$$

Range of x-values $x_u \leq x \leq x_1$

In this range of x-values $C_b \geq 0.99$ and the definitions for the various BLs are:

$$\delta_b = 0 \quad where \quad C = 0.99; \quad \delta_u = y \quad where \quad C = 0.5; \quad \delta = y \quad where \quad C = 0.01;$$

$$\delta_0 = y \quad where \quad C = 0.001 \tag{54}$$

Range of x-values $x \geq x_1$

In this range of x-values $C_b < 0.99$ and the definitions for the various BLs are:

$$\delta_b = 0; \quad \delta_u = y \quad where \quad C = 0.5C_b; \quad \delta = y \quad where \quad C = 0.01;$$

$$\delta_0 = y \quad where \quad C = 0.001C_b \tag{55}$$

The definitions of the various BLs given by eqs. (50)-(55) are practically identical to those given in the preceding section. However, they allow performance of tests needed to justify the top specified boundary layer (TSBL) approach. Such tests also provide values of the power coefficients n_i $(i=3,...,6)$ which characterize the salinity distribution in ranges of x-values referring to the saltwater mound and its downstream region. Details concerning these analyses are given in following paragraphs.

The numerical experiments covered a wide range of values of the variables a, x_e and q_R. In Fig. 4 we present some results exemplifying the methodology of our calculations, which are later used for supplying basic information needed by the TSBL approach. Results of this figure refer to $x_e = 100$, $q_R = 0.1$ and various values of a, which

are relevant to the formation of saltwater mounds. Values of this parameter larger than considered in Fig. 4 do not lead to the development of the saltwater mound. It should be noted that, as shown in Fig. 4, due to the comparatively high values of q_R/a the range of x-values smaller than $x_{0.5}$ is very small and can be neglected in our calculations of the development of the BLs along the horizontal coordinate.

Figure 4(a) refers to the highest value of a considered in our numerical simulations (i.e. $a = 0.02$), and Figs. 4(c) and 4(d) refer to the lowest value of this parameter (i.e. $a = 0.005$). It should be noted that considering $l_0 = 1$ m, *Garneau (1995)* calculated dispersivities of such range of values in south central Kansas. However, in most practical cases higher values of the transverse dispersivity are expected. For the lowest value of a, the build-up of the saltwater mound starts at lowest x-value. Furthermore the saltwater mound maximum thickness is larger, and its length is very much larger than for the highest value of a. In all examples given by Fig. 4, identical quantities of salt seep into the aquifer, as $q_R = 0.1$ in all these examples. Therefore, differences in salinity distributions are solely attributed to differences in the transverse dispersivity. Downstream of $x = x_e$, the only parameter that causes variations in the salinity distribution is the transverse dispersivity. Therefore, although the rate of development and expansion of the saltwater mound is not very sensitive to the value of a, the rate of decrease of the thickness of the saltwater mound is very sensitive to the value of this parameter.

We define a variable δ_R, which is given by

$$\delta_R = \frac{\delta_0 - \delta_u}{\delta_u - \delta_b} \tag{56}$$

Values of this parameter were calculated for the whole horizontal extent of the simulated domains shown in Figs. 4(a) - (c). As indicated by eq. (C5) δ_R should be connected to the ratio between the power coefficients n_4 and n_3 characterizing the salinity distribution in the transition zone between the saltwater mound and the freshwater zone. However, it should be noted that eq. (C5) is also applicable downstream of the saltwater mound with regard to vanishing values of δ_b and power coefficients n_6 and n_5. Therefore,

eq. (56) can also be useful downstream of the saltwater mound region to identify the possible ratio between n_6 and n_5.

Figure 5(a) is based on the analysis of the data represented in Figs. 4(a) - (c). We have calculated values of δ_R to identify the appropriate ratio between the power coefficients for x-values associated with the development of the saltwater mound (i.e. n_4 and n_3) as implied by eq. (C5). Figure 5(a) shows that in the region of the saltwater mound this ratio is about 1.5. However, the saltwater mound affects the ratio of power coefficients for x-values downstream of the saltwater mound (i.e. n_6 and n_5). *Rubin and Buddemeier (1998d)* found that the ratio between n_6 and n_5 is about 2.17. With a = 0.02, as shown in Fig. 4(a), the saltwater mound is extended between x = 50 and x = 200. Figure 5(a) shows that the ratio between n_6 and n_5 for a = 0.02 increases downstream of the saltwater mound and gradually approaches the expected value typical of the range of $x > x_1$. However, even a long distance downstream of the saltwater mound this ratio is still smaller than the value of 2.17 expected in the absence of a saltwater mound. Therefore, we performed another set of numerical simulations for a larger horizontal extent of the simulated domains and used the numerical results for the calculation of δ_R as shown in Fig. 5(b). The following calculations evaluate the quantitative effect of this phenomenon on the development of BLs downstream of x_1.

Figure 6 is also based on the analysis of data represented in Fig. 4 and similar simulations. We use a new type of normalized vertical coordinate ζ defined for the whole transition zone, between the saltwater mound and the freshwater, as

$$\zeta = 1 - \xi \quad at \quad \delta_b \le y \le \delta_u \tag{57}$$

$$\zeta = 1 + \eta \quad at \quad \delta_b \le y \le \delta_0 \tag{58}$$

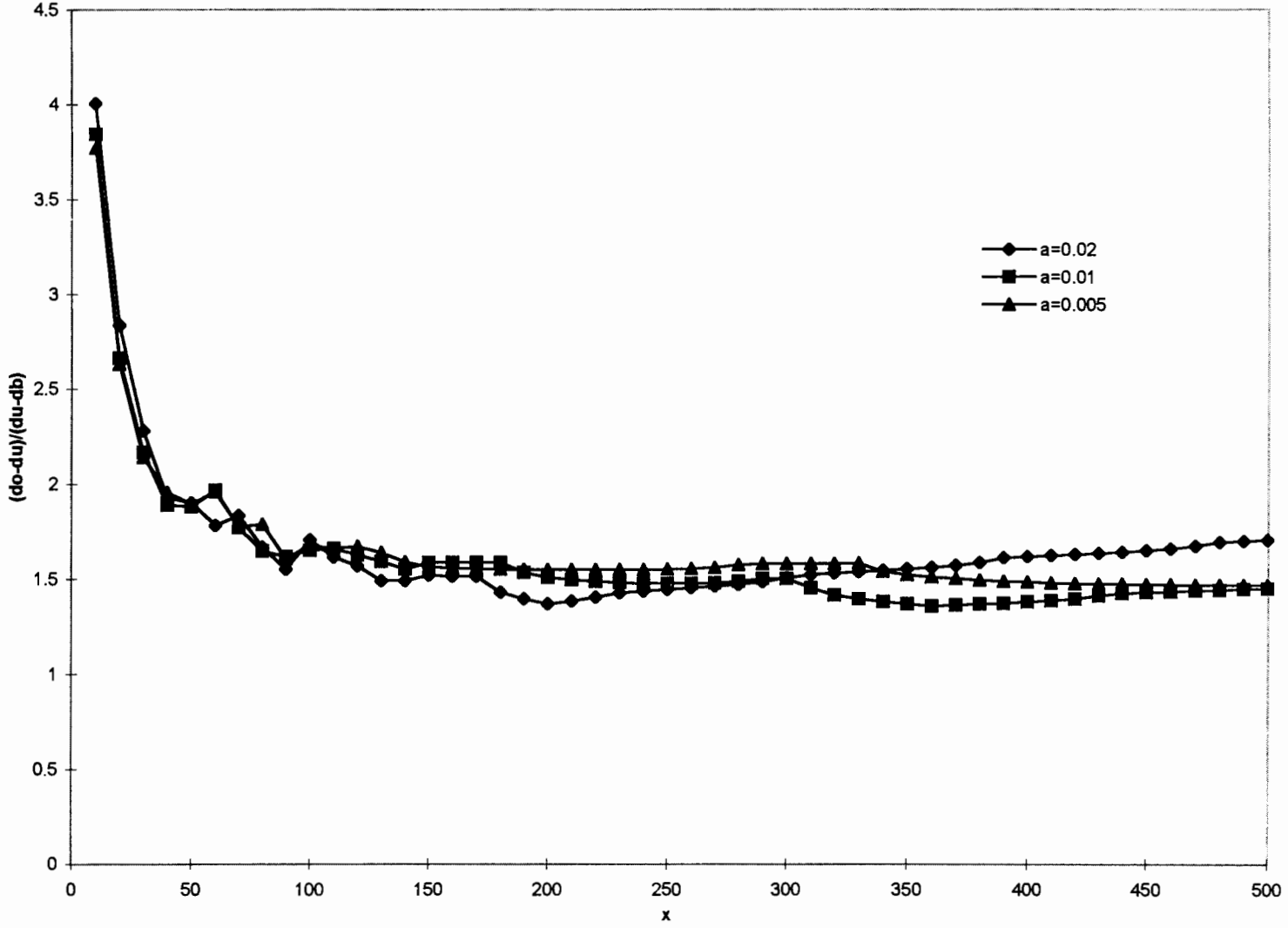

Figure 5a Variation of the ratio between thickness of the outer and inner BLs (δ_R) along the longitudinal (x) coordinate ($q_R = 0.1$, $x_e = 100$)

(a) $x_{max} = 500$

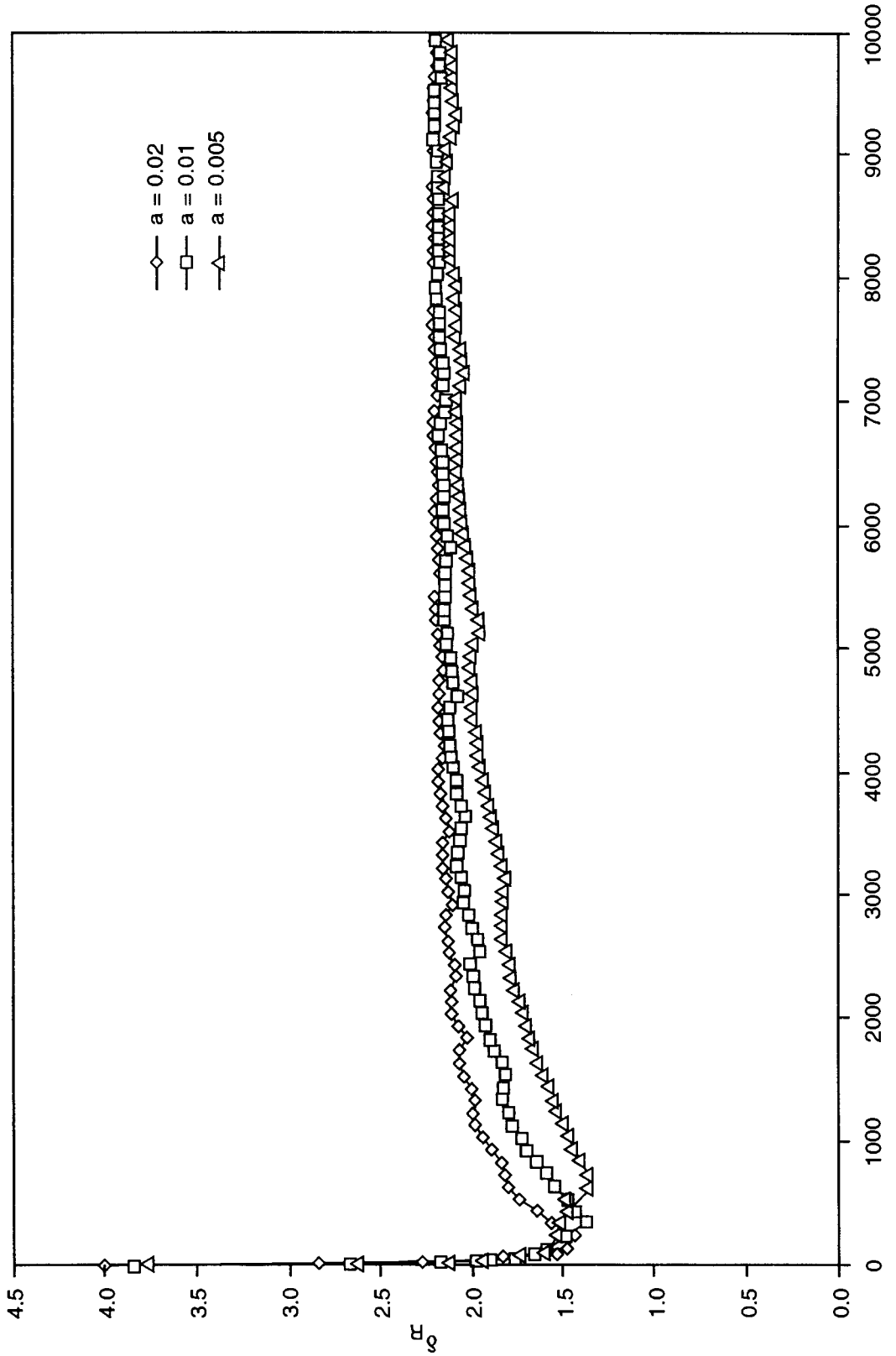

Figure 5b Variation of the ratio between thickness of the outer and inner BLs (δ_R) along the longitudinal (x) coordinate ($q_R = 0.1$, $x_e = 100$)

(b) $x_{max} = 10000$

Therefore, ζ varies between $\zeta = 0$ and $\zeta = 2$ while covering the thickness of the transition zone. In Fig. 6 we represent numerous profiles of salinity distribution C versus ζ various x-values in the region of the saltwater mound. It should be noted that the numerical simulations indicate that for $a = 0.005$ the downstream end of the saltwater mound is at about $x = 5000$. However, as the thickness of the saltwater mound downstream of x-value approximately 700 is very small, Fig. 4(d) gives the impression that at an x-value of approximately 700 the saltwater mound vanishes. Figures 6(a) - (d) refer to saltwater mound regions typical of several values of the transverse dispersivity. These figures show that all normalized salinity profiles in the transition zone between the saltwater mound and the freshwater zone shrink to a single curve, which is identical for all values of a considered.

Introducing the vertical coordinate ζ into eqs. (35) and (36), respectively, we obtain the following expressions for the salinity distributions in the transition zone developed between the saltwater mound and the freshwater zone

$$C = 1 - 0.5\zeta^{n_3} \quad at \quad 0 \le \zeta \le 1 \quad (\delta_b \le y \le \delta_u) \tag{59}$$

$$C = 0.5(2 - \zeta)^{n_4} \quad at \quad 1 \le \zeta \le 2 \quad (\delta_u \le y \le \delta_0) \tag{60}$$

These expressions are applicable to the range of x-values: $x_u \le x \le x_1$.

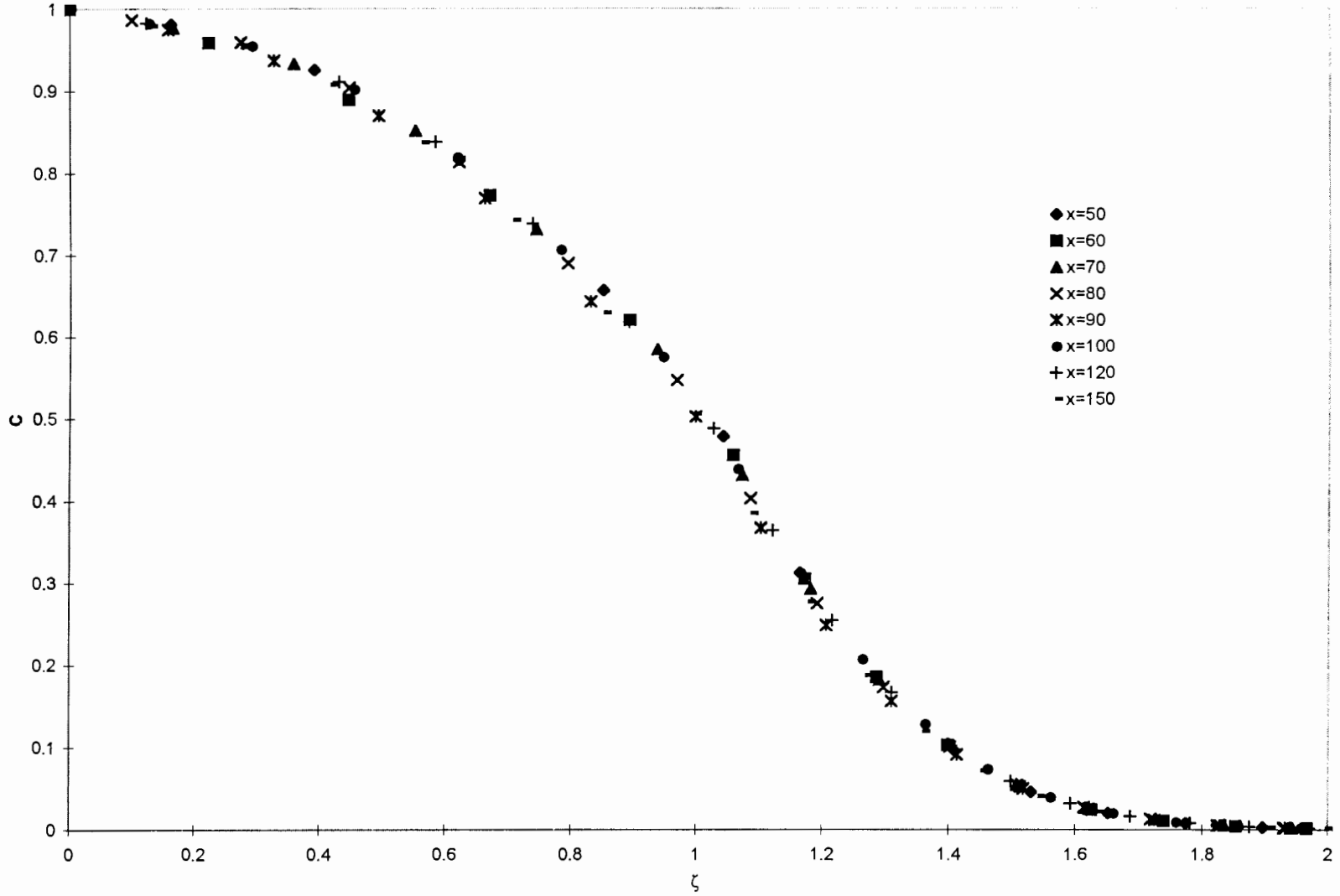

Figure 6a Profiles of C versus the modified vertical coordinate ζ in the transition zone built-up on top of the saltwater mound ($q_R = 0.1$, $x_e = 100$)

(a) $a = 0.01$; $50 \leq x \leq 150$

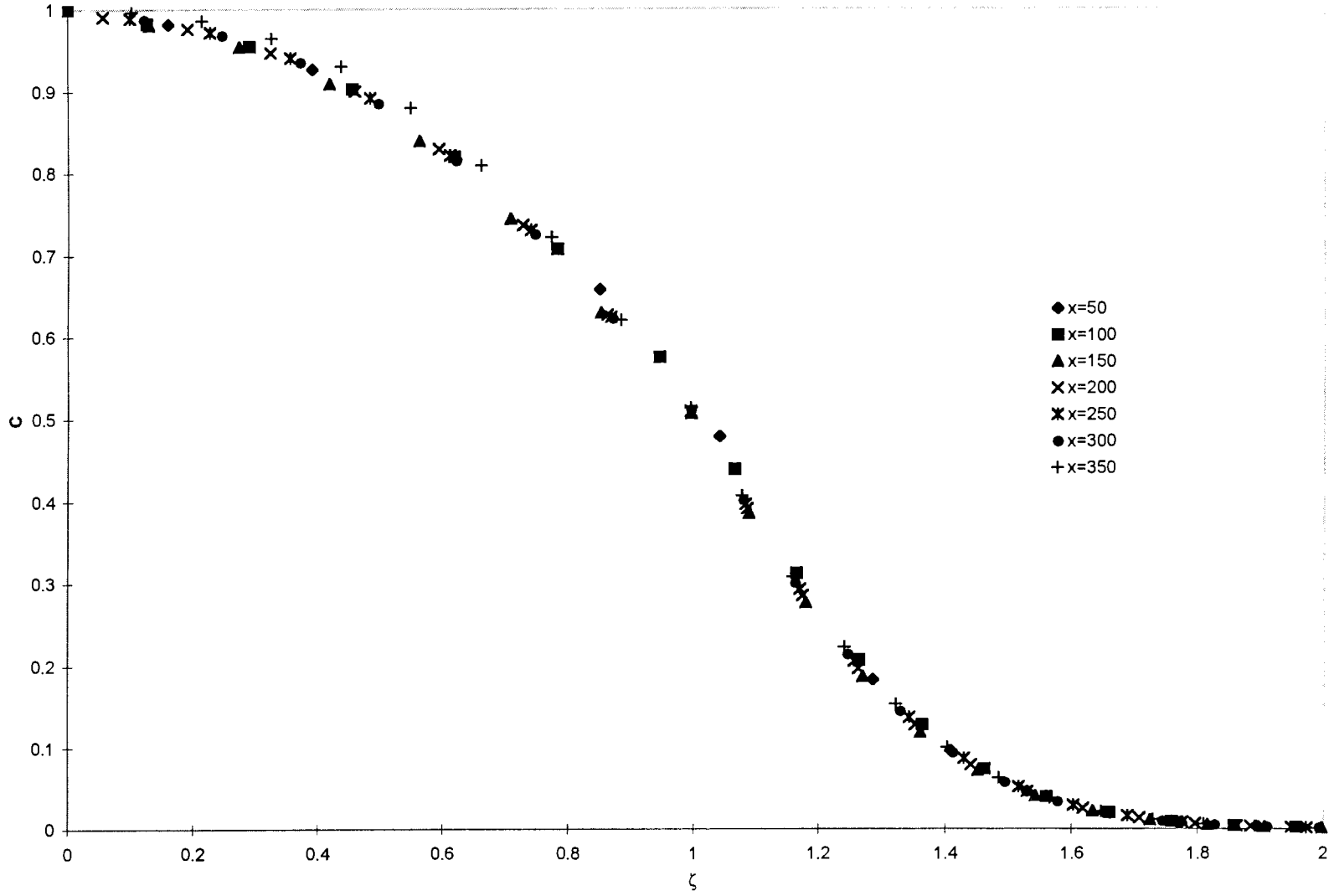

Figure 6b Profiles of C versus the modified vertical coordinate ζ in the transition zone built-up on top of the saltwater mound ($q_R = 0.1$, $x_e = 100$)

(b) $a = 0.01$; $50 \leq x \leq 350$

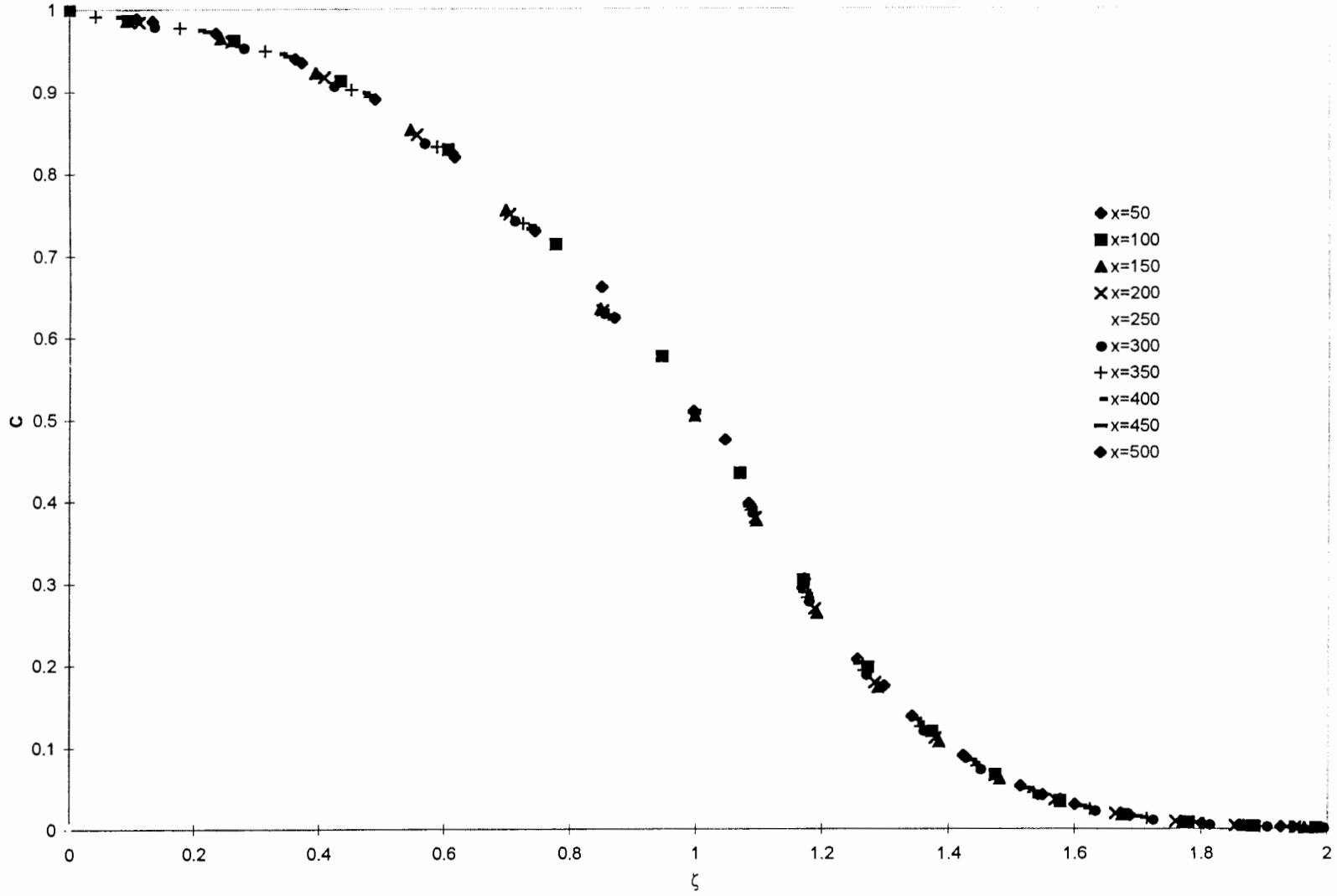

Figure 6c Profiles of C versus the modified vertical coordinate ζ in the transition zone built-up on top of the saltwater mound ($q_R = 0.1$, $x_e = 100$)

(c) $a = 0.005$; $50 \le x \le 500$

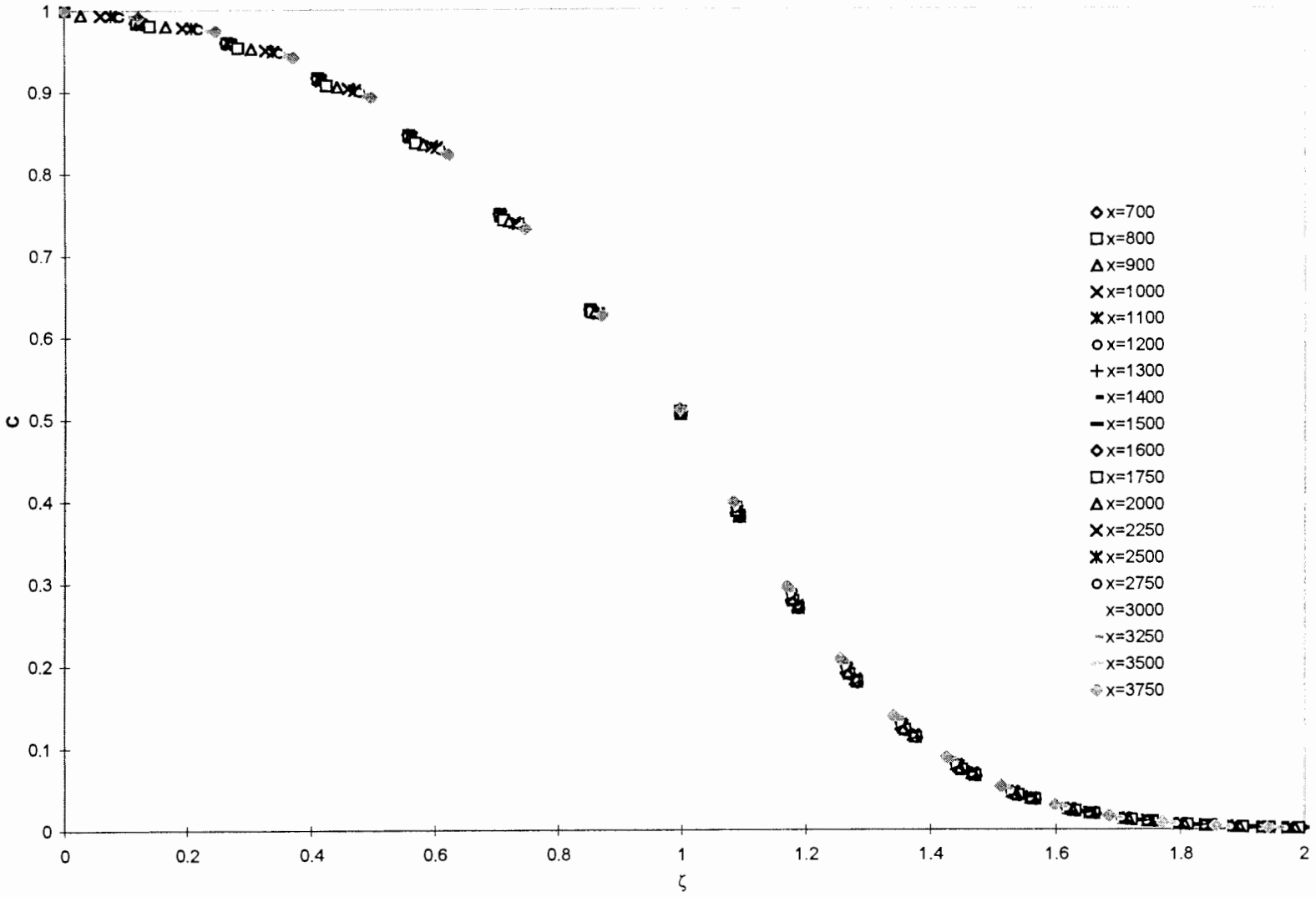

Figure 6d Profiles of C versus the modified vertical coordinate ζ in the transition zone built-up on top of the saltwater mound ($q_R = 0.1$, $x_e = 100$)

(d) $a = 0.005$; $700 \leq x \leq 3750$

Figure 7(a) demonstrates the use of these expressions and the data given in Figs. 5(a) and 6(b) for the determination of appropriate values of n_3 and n_4. Considering the results given in Fig. 5(a), we assume that the ratio between these two power coefficients is about 1.5. In Fig. 7(a) we compare the data of Fig. 6(b) with two examples of power series representing the salinity distributions in the transition zone: n_3, n_4 = 2, 3, and n_3, n_4 = 2.7, 4. It is clearly that the example of n_3, n_4 = 2, 3 provides a better fit of eqs. (59) and (60) to the data of Fig. 6(b). However, as indicated by Figs. 4(d) and 5(b), in cases of very low values of a (e.g. a = 0.005) the decrease the saltwater mound thickness is extended along a very large horizontal extent, over which the value of δ_R gradually increases. Figure 7(b) compares some power series expansions with the normalized salinity profiles for a very large range of x-values. It seems that n_3, n_4 = 2, 3 is also a good approximation in this case. Therefore, we may consider that appropriate values of n_3 and n_4 should be *2* and *3*, respectively.

In Figs. 8 and 9 we evaluate possible effects of the saltwater mound on salinity distribution in cross sections located downstream of the saltwater mound. Both figures refer to x-values larger than x_1. For this region of x-values we again apply the coordinate ζ whose definition is given by eqs. (59) and (60), with δ_b =0.

Fig, 8(a) refers to a = 0.01, and Fig. 8(b) refers to a = 0.005. In both cases, we calculate values of the normalized salinity profiles (i.e. C/C_b versus ζ). Both figures indicate that all normalized salinity profiles shrink to a single curve.

Introducing the coordinate ζ into eqs. (41) and (42), respectively, while considering c_r = 0.5, we obtain

$$C / C_b = 1 - 0.5\zeta^{n_5} \quad at \quad 0 \le \zeta \le 1 \quad (0 \le \delta_u) \tag{61}$$

$$C / C_b = 0.5(2 - \zeta)^{n_6} \quad at \quad 1 \le \zeta \le 2 \quad (\delta_u \le y \le \delta_0) \tag{62}$$

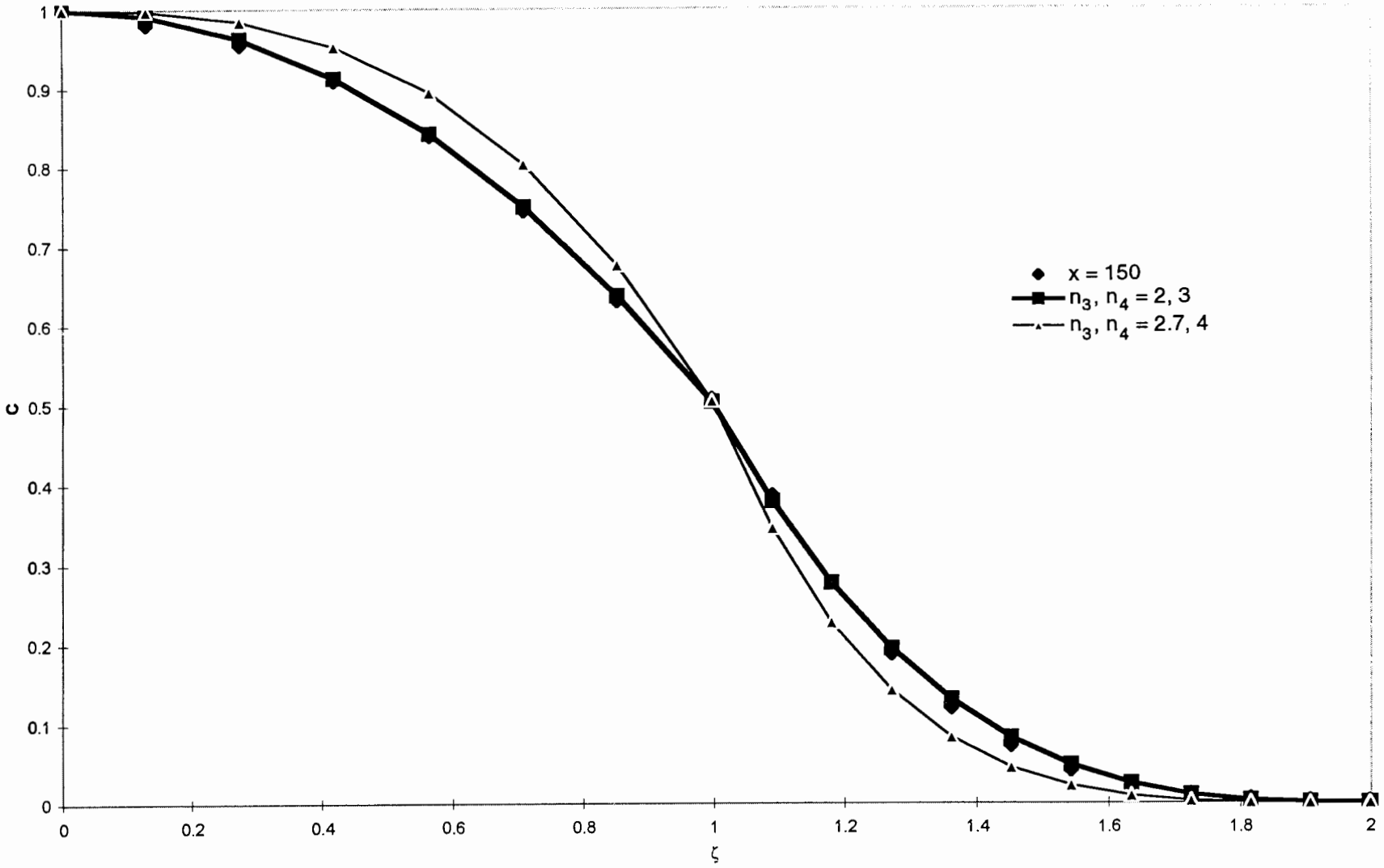

Figure 7a Fitting of power series expansion to the normalized salinity profiles of the transition zone built-up on top of the saltwater mound ($q_R = 0.1$, $x_e = 100$)

(a) $a = 0.01$

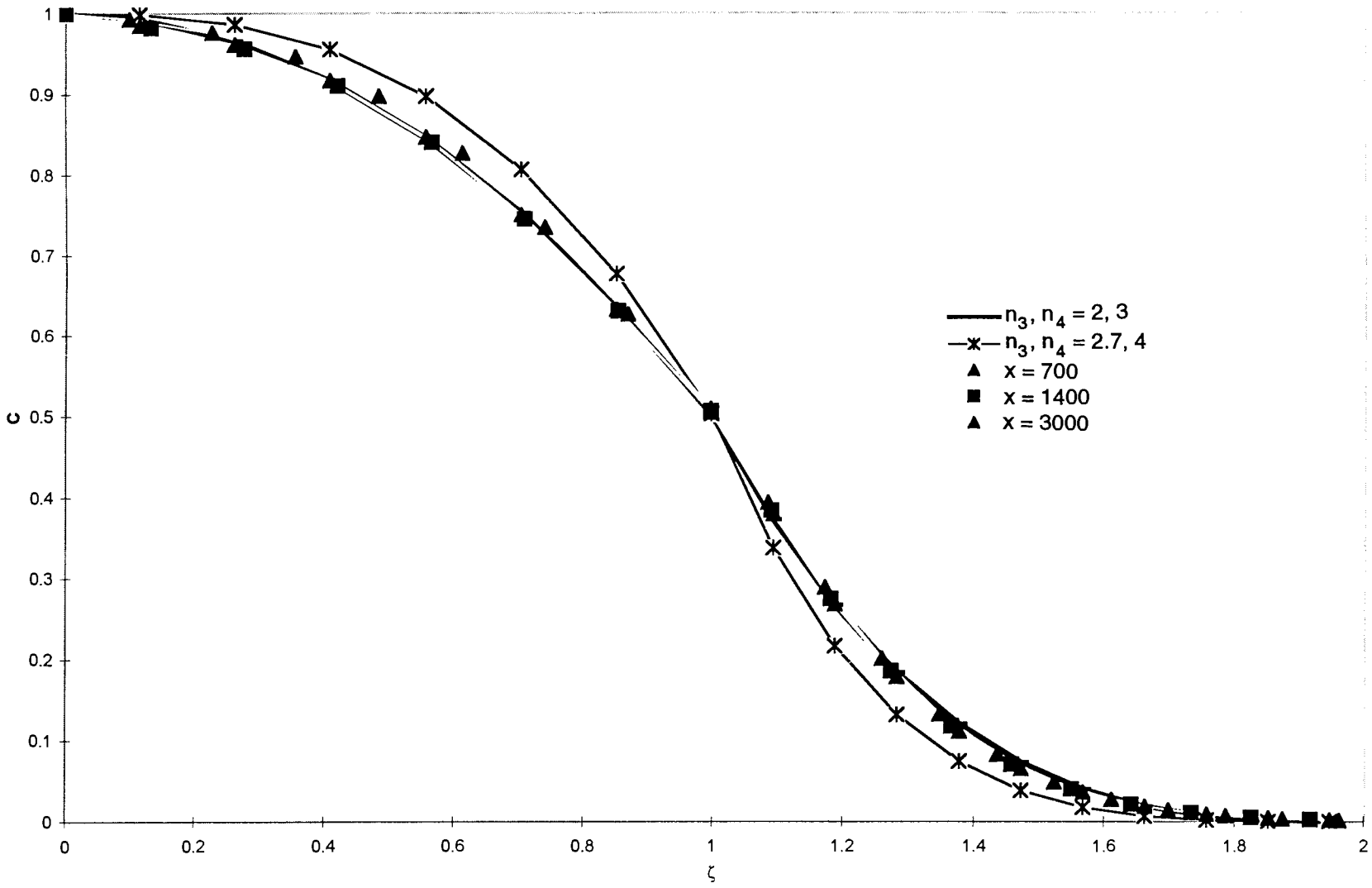

Figure 7b Fitting of power series expansion to the normalized salinity profiles of the transition zone built-up on top of the saltwater mound ($q_R = 0.1$, $x_e = 100$)

(b) $a = 0.005$

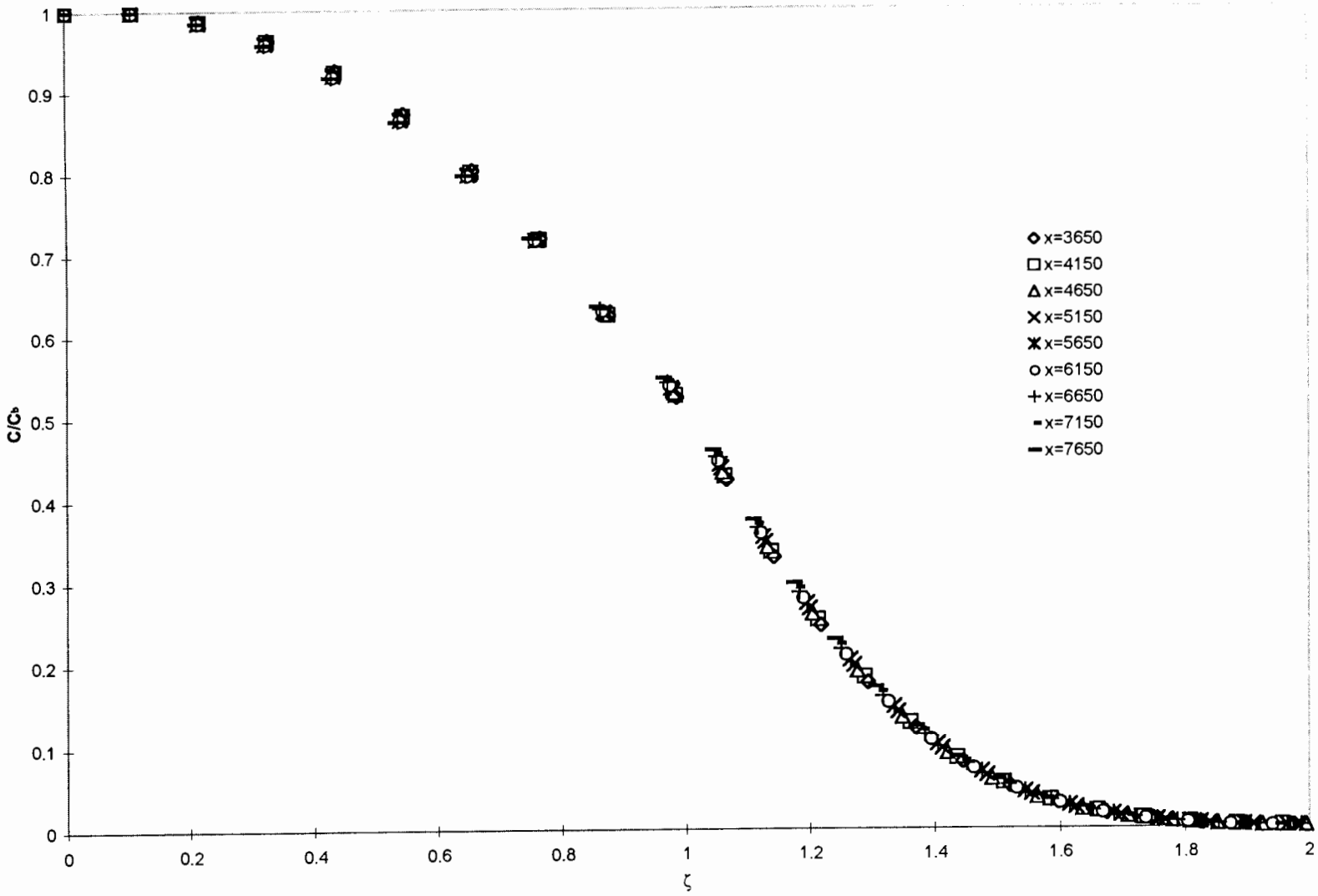

Figure 8a Profiles of C/C_b versus the modified coordinate ζ in the transition zone developed downstream of the saltwater mound ($q_R = 0.1$, $x_e = 100$)

(a) $a = 0.01$

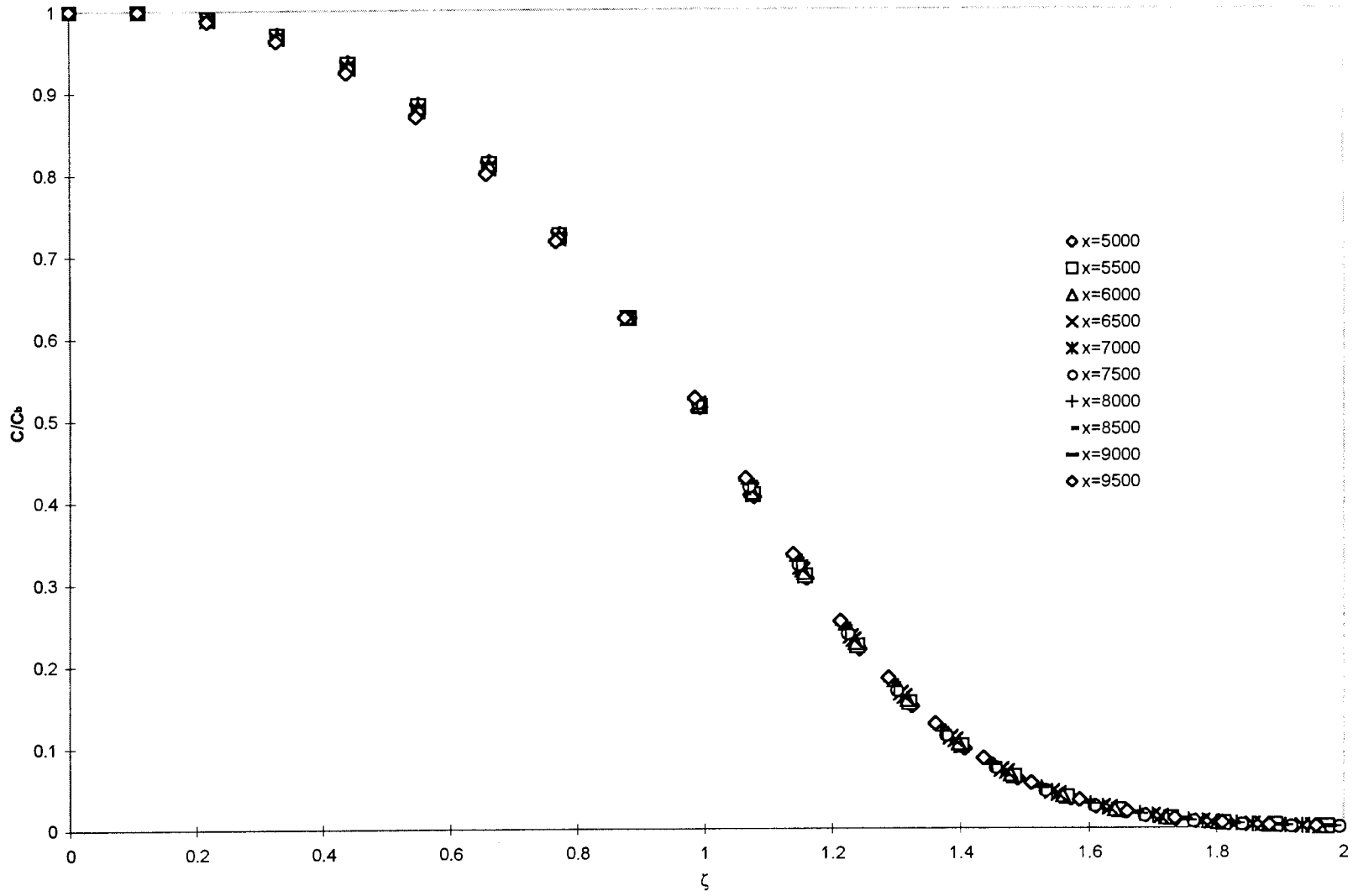

Figure 8b Profiles of C/C_b versus the modified coordinate ζ in the transition zone developed downstream of the saltwater mound ($q_R = 0.1$, $x_e = 100$)

(b) $a = 0.005$

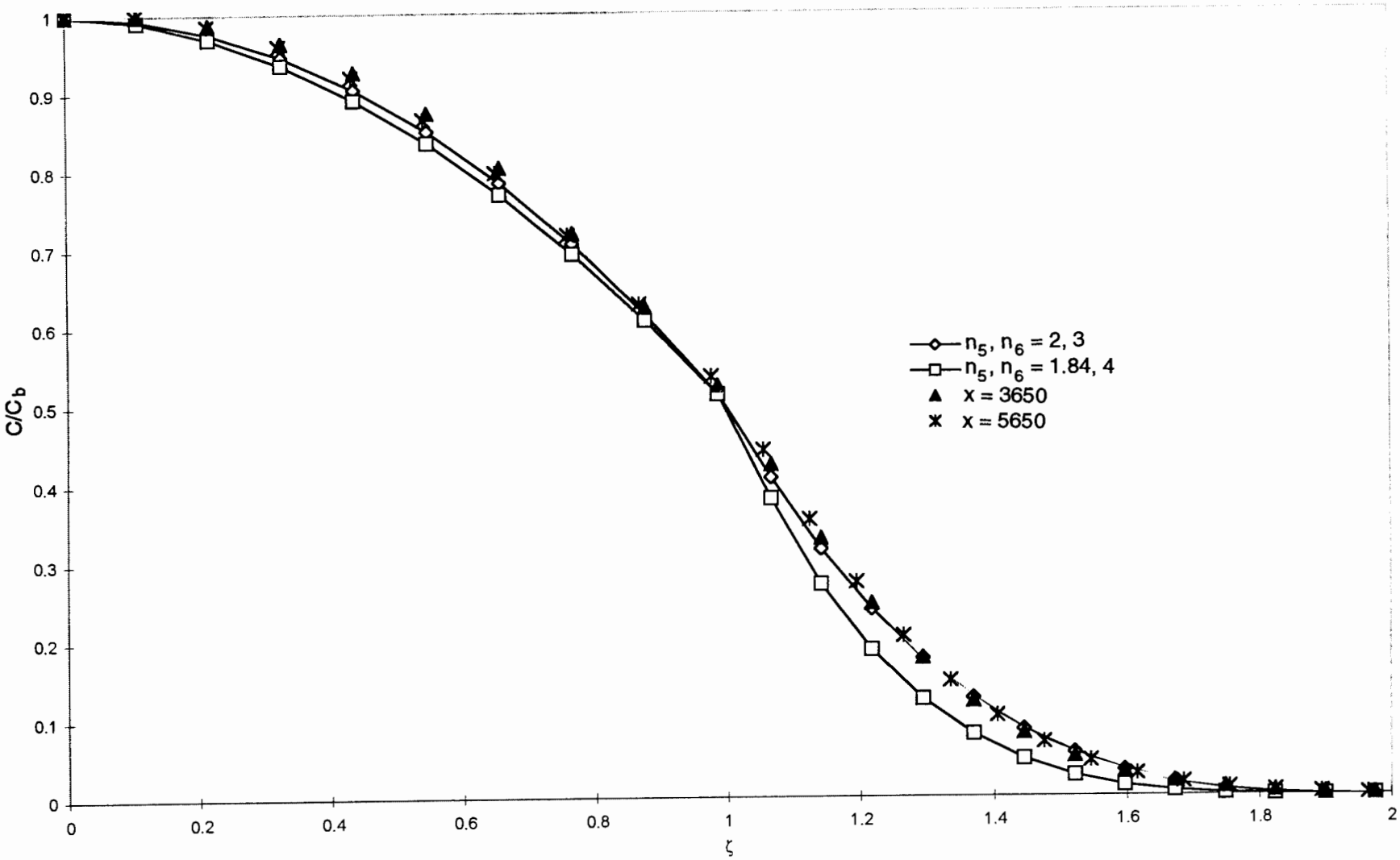

Figure 9a Fitting of power series expansions to the normalized salinity profiles of the transition zone built-up downstream of the saltwater mound ($q_R = 0.1$, $x_e = 100$)

(a) $a = 0.01$

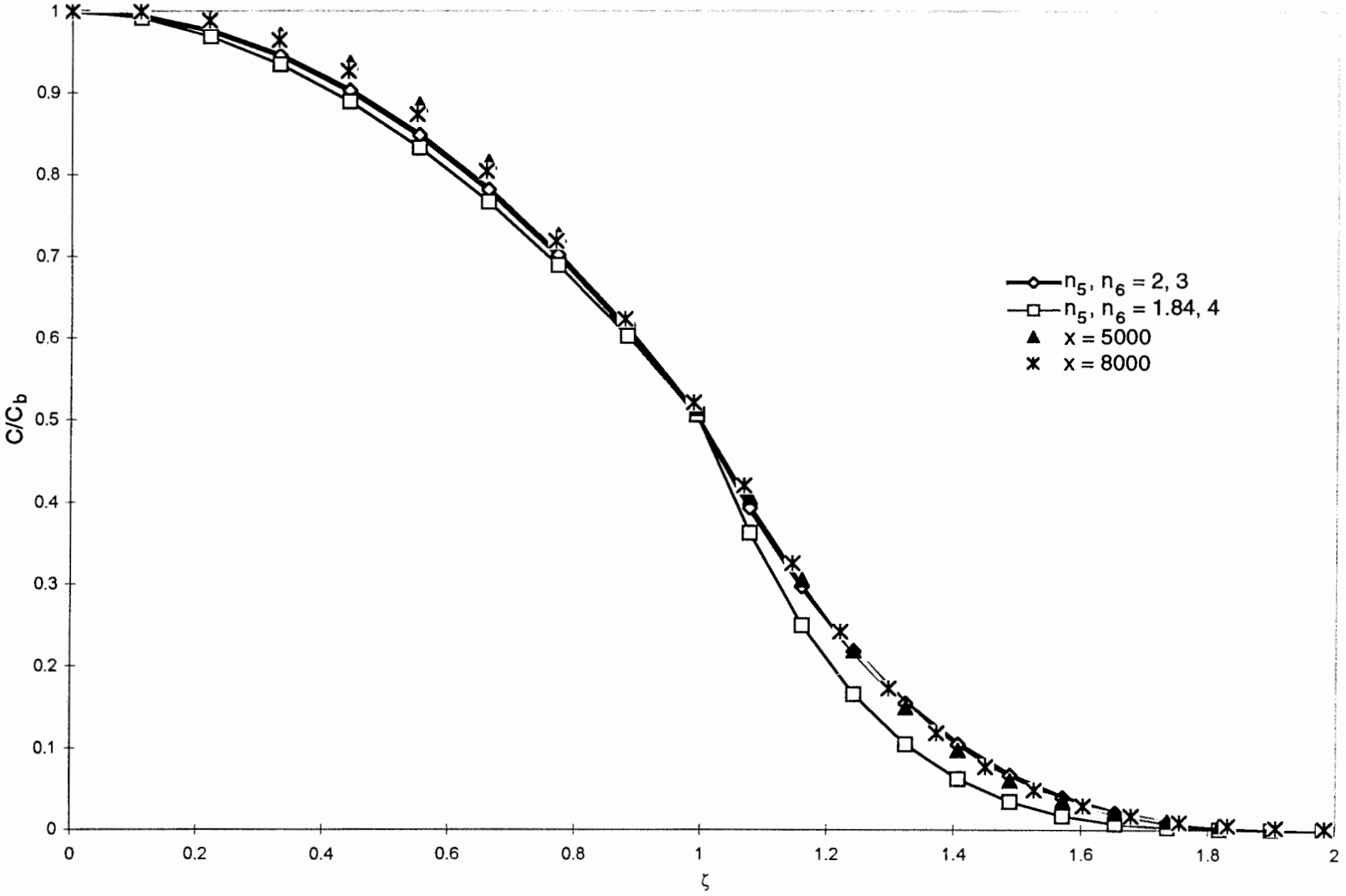

Figure 9b Fitting of power series expansions to the normalized salinity profiles of the transition zone built-up downstream of the saltwater mound ($q_R = 0.1$, $x_e = 100$)

(b) $a = 0.005$

In Fig. 9 we compare values of the normalized salinity profiles taken from Fig. 8 with two examples of power series expansions. We consider two examples: n_5, n_6 = 2, 3 (as used in the range $x_u \leq x \leq x_1$) and n_5, n_6 = 1.84, 4 as implied by the study of *Rubin and Buddemeier (1998c)*. Downstream of the saltwater mound it seems that the use of n_5, n_6= 2, 3 also provides a better fit to the numerically calculated salinity profiles. This indicates that the effect of the saltwater mound buildup is extends a very large distance downstream of the saltwater mound location.

Calibration and application of the TSBL method

Following determination of the power coefficients n_i $(i = 3,...6)$ it is possible to apply the top specified boundary layer (TSBL) with no calibration and obtain results which are quite good for practical purposes. However, the preliminary tests only indicated that we can define in the domain regions of so-called "similar salinity profiles". We have identified the laws of similitude governing these regions. Therefore we have justified the use of the BL approach for the determination of salinity distribution in the domain, provided that values of the thickness of the various BLs are correct. For determination of the thickness values of the various BLs, as well as the thickness of the saltwater mound, we developed expressions that approximately satisfy the principle of mass conservation. In the range of x-values occupied by the impermeable layer discontinuity, changes in the aquifer discharge due to the saltwater seepage are ignored. In our numerical calculations we considered such changes, while assuming that the aquifer thickness is 80 length units. Although changes in the aquifer discharge can be incorporated in the TSBL method, they may require the use of numerical calculations that we have tried to avoid in order to obtain quick and very simple expressions for the thickness of BLs. In the saltwater mound region, the BLs are built around the floating boundary represented by the isohaline C = 0.5. According to the TSBL method of approximation, there is no salinity transfer between the saltwater mound and the inner BL. Under such conditions, the inner BL cannot grow on account of the saltwater mound, and the saltwater mound can never decay. We have

overcome this difficulty by applying the integral mass balance as given in eq. (37). However, the numerical calculations have indicated that only about 85 percent of the salinity introduced into the aquifer is transferred through the transition zone. There have also been some discrepancies of mass balance with our numerical model. However, we demonstrate in this section how to calibrate the TSBL method to better fit some numerical simulation results.

In the following paragraph we evaluate and interpret the use of each calibration coefficient. The calibration coefficients α_1 and α_2 of eqs. (38) and (39) are applied to compensate for the neglect of effects of the seeping saltwater discharge on the aquifer discharge. The increased discharge has some effect on the salinity distribution in the domain. The coefficients α_3 and α_4 of eqs. (37) and (40) scale the possible development of the BLs in response to the saltwater mound buildup. We have applied in eq. (37) a single calibration coefficient, α_3, which is associated with the most significant term. In eq. (40) we introduce the coefficient α_4 which is associated with the remaining terms where there is no saltwater seepage. Coefficients α_5 and α_6 represent the relationships between average salinity gradients in the inner and outer BLs and the development of these layers *(Rubin and Buddemeier, 1998c).*

Figure 10 demonstrates the process of the TSBL calibration. In each range of x-values we have chosen values of calibration coefficients that provide the best fit to numerically calculated values of the various values of the BL thickness. Although such a determination can be made by various sophisticated methods, these examples are based on quick calculations and graphical presentations. Agreement between the numerical and TSBL results is quite good, as shown in Figs. 10(a) and 10(b) which refer to $a = 0.01$. Identical values of the calibration coefficients were used to obtain Fig. 10(c), which refers to $a = 0.05$. The agreement between the numerical and TSBL results in this figure is also good. After calculation of the development of the saltwater mound and the various BLs, predicted values of C_b versus x obtained by using the numerical simulations and the TSBL method were compared as shown in Fig. 11. The agreement between values predicted by both methods is quite good. As expected, a better fit is obtained in the case of $a = 0.01$ than in the case of $a = 0.005$, as the calibration has been performed with $a = 0.01$.

Values of the calibration coefficients applied to calculations associated with Figs. 10 and 11 are:

$$\alpha_1 = 15.5; \quad \alpha_2 = 4.25; \quad \alpha_3 = 0.8 \quad at \quad x_u \le x \le x_e \tag{63}$$

$$\alpha_1 = 7; \quad \alpha_2 = 0.83; \quad \alpha_4 = 0.8 \quad at \quad x_e \le x \le x_1 \tag{64}$$

$$\alpha_5 = 0.8; \quad \alpha_6 = 0.62 \quad at \quad x_1 \le x \le x_1 + 300 \tag{65}$$

$$\alpha_5 = 1.0; \quad \alpha_6 = 0.7 \quad at \quad x_1 + 300 \le x \le x_{\max} \tag{66}$$

where x_{max} is the horizontal extent of the simulated domain.

It should be noted that values of α_3 and α_4 are identical and close to unity. Therefore, it was possible to apply α_3 as a calibration coefficient multiplying all right hand side terms of eq. (37).

Besides determination of the variation of the best-fit coefficients of the BL modeling, as shown by eqs. (63) – (66), adjustment of quantities characterizing the BL also should be done at each interface between adjacent ranges of x-values. Appendix E provides details about such adjustments.

It should be noted that values of the calibration coefficients specified in eqs. (63) - (66) have been obtained from visual experiments. Superior values might be obtained by use of a better curve fitting method. However, eqs. (63) - (66) represent the correct magnitudes of the calibration coefficients. *Rubin and Buddemeier (1998c)*, considered small values of q_R/a and no buildup of the saltwater mound, obtained values very close to those given by eq. (66).

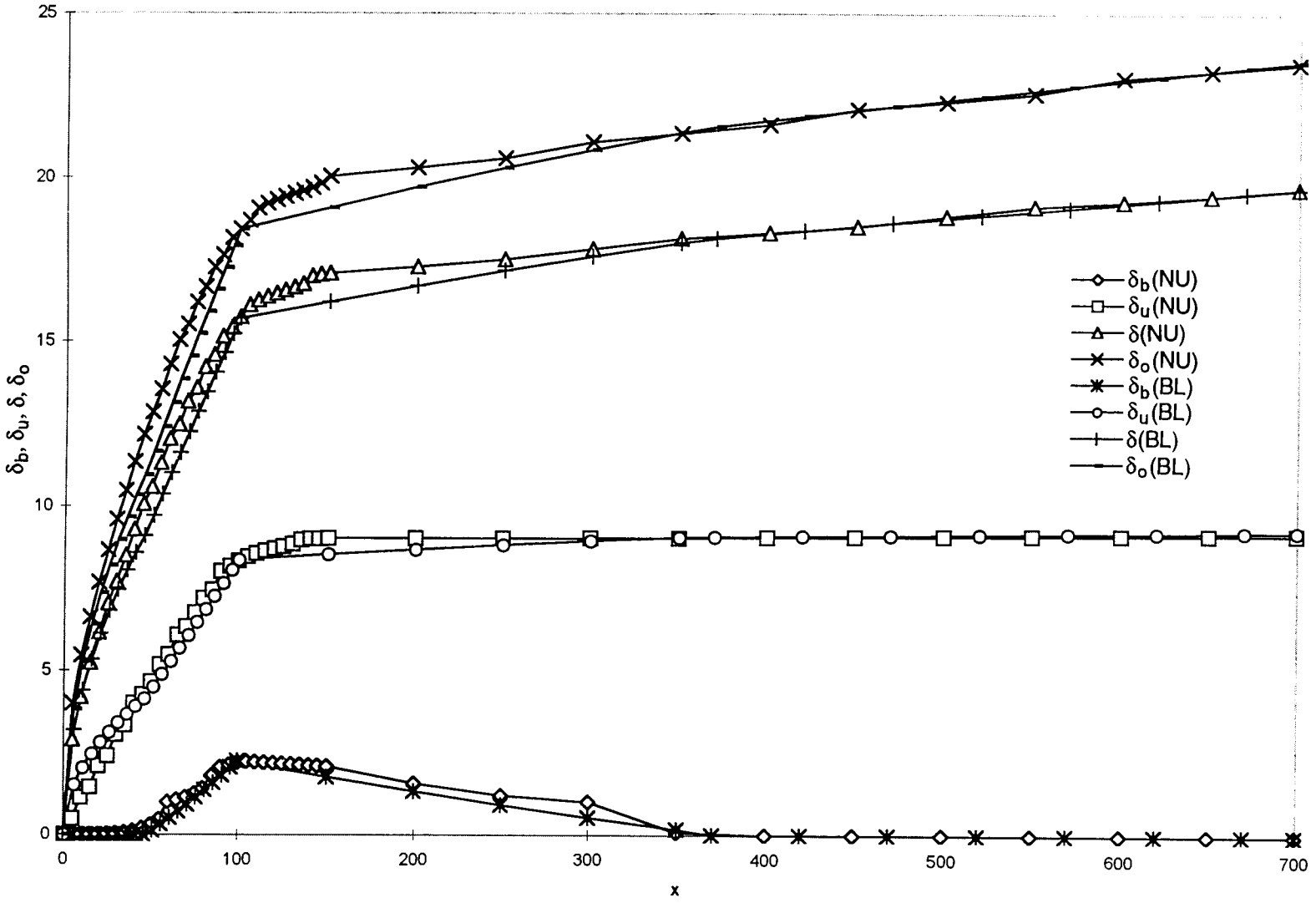

Figure 10a Calibration and application of the TSBL method by comparing the TSBL results with rigorous numerical simulations ($q_R = 0.1$, $x_e = 100$)

(a) a=0.01; x_{max}=700

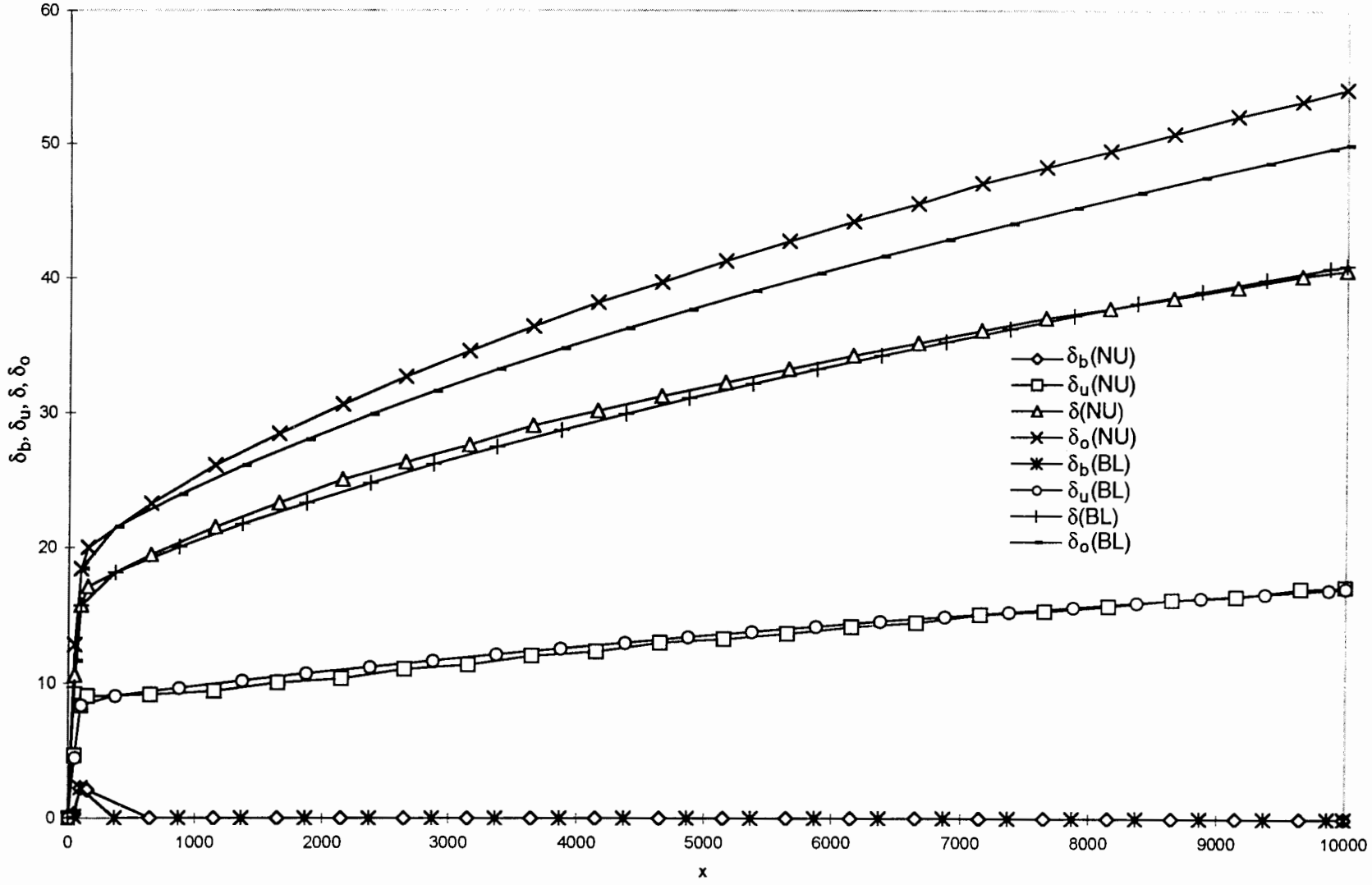

Figure 10b Calibration and application of the TSBL method by comparing the TSBL results with rigorous numerical simulations ($q_R = 0.1$, $x_e = 100$)

(b) *a=0.01;* x_{max}*=10000*

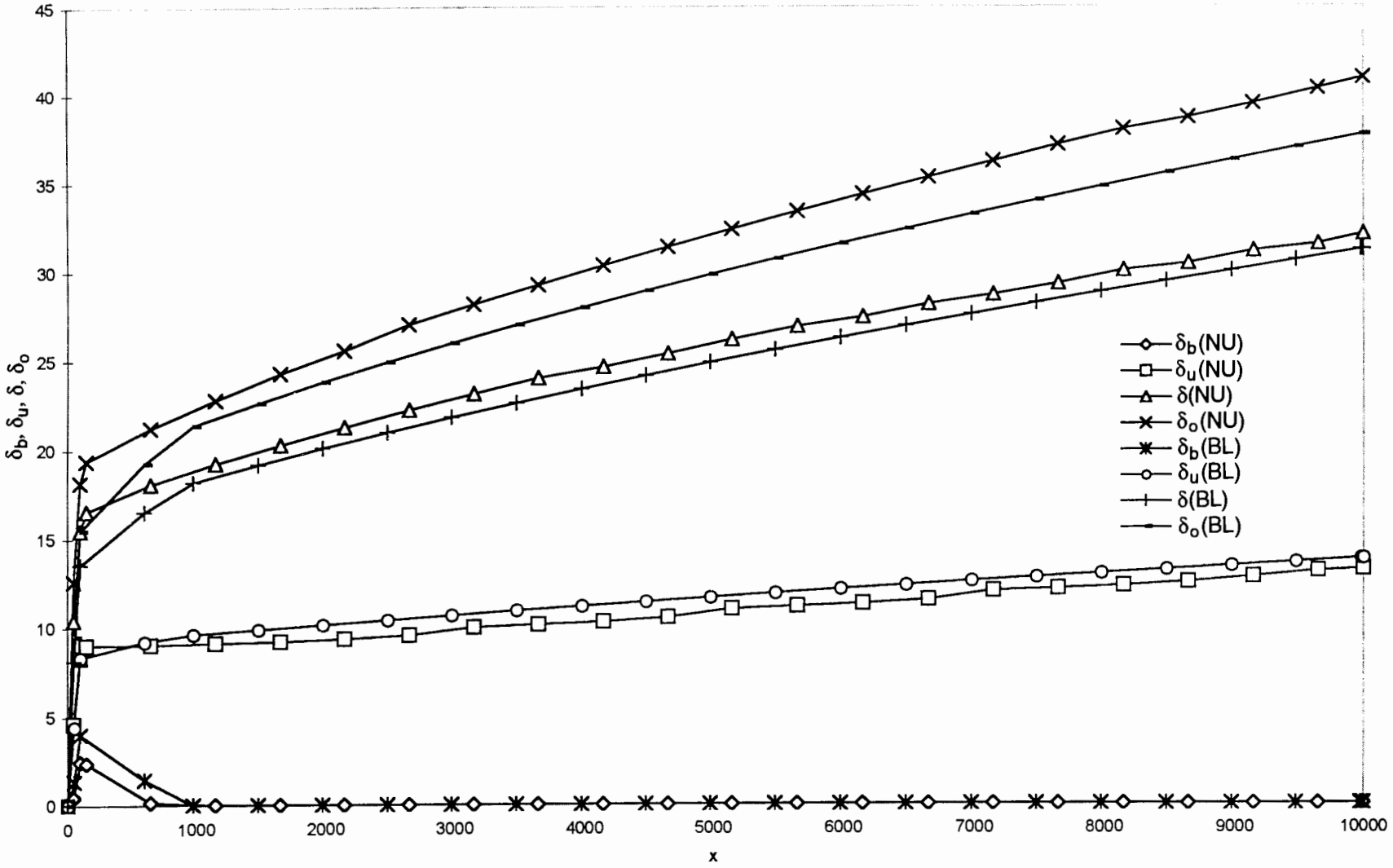

Figure 10c Calibration and application of the TSBL method by comparing the TSBL results with rigorous numerical simulations ($q_R = 0.1$, $x_e = 100$)

(c) $a = 0.005$; $x_{max} = 10000$

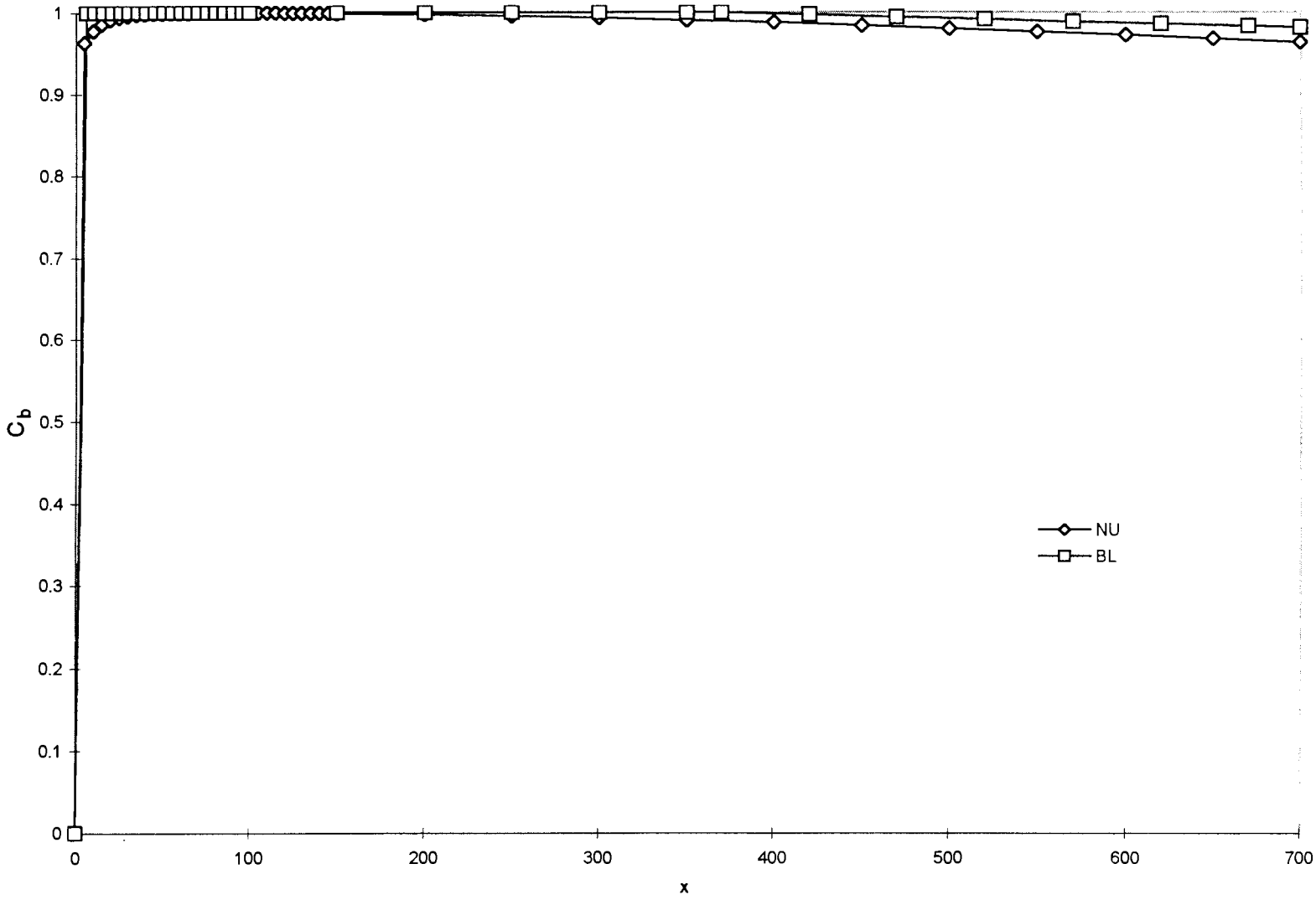

Figure 11a Comparison between values of C predicted by the TSBL method and rigorous numerical simulations ($q_R = 0.1$, $x_e = 100$)

(a) $a = 0.01$; $x_{max} = 700$

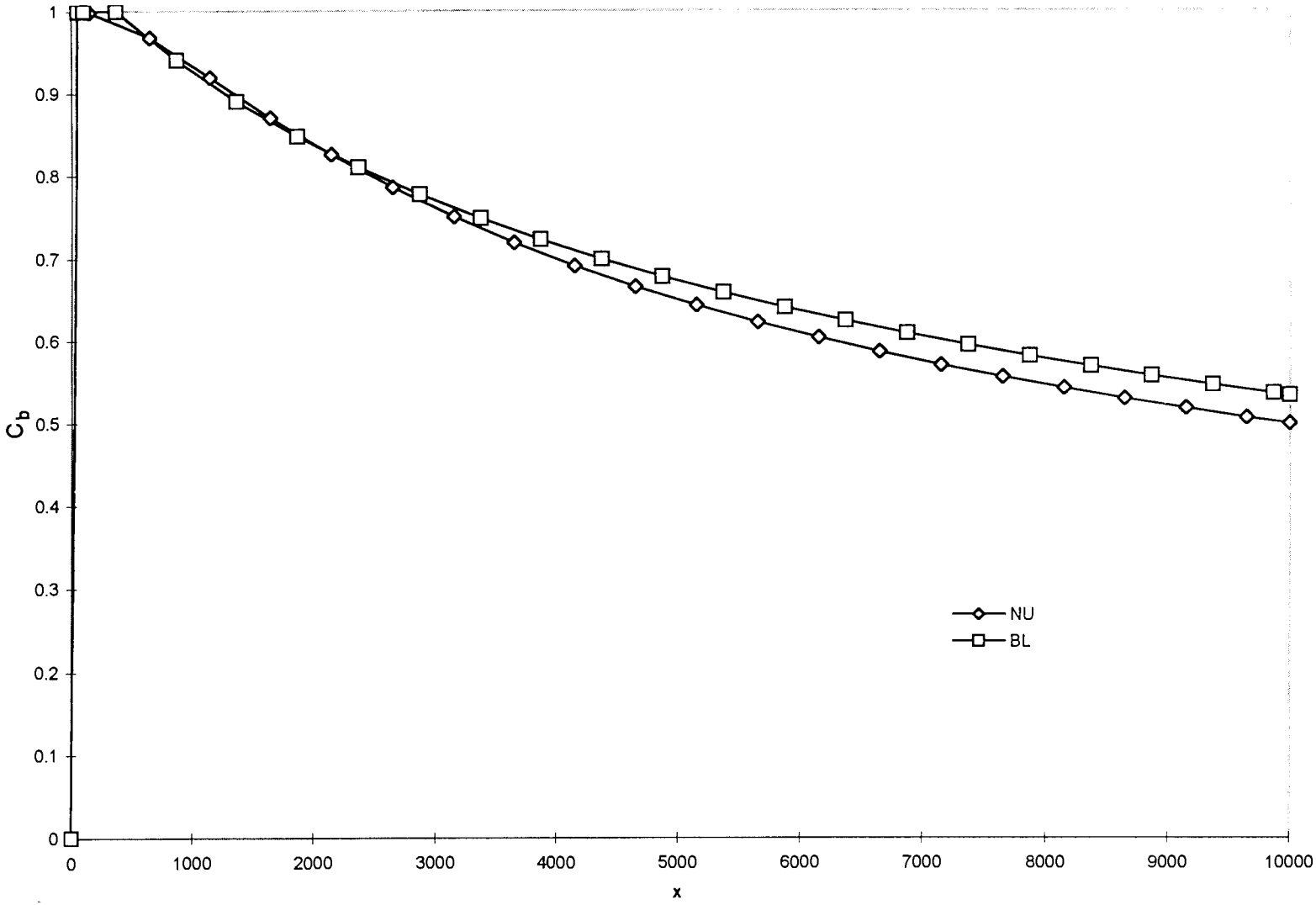

Figure 11b Comparison between values of C predicted by the TSBL method and rigorous numerical simulations ($q_R = 0.1$, $x_e = 100$)

(b) $a = 0.01$; $x_{max} = 10000$

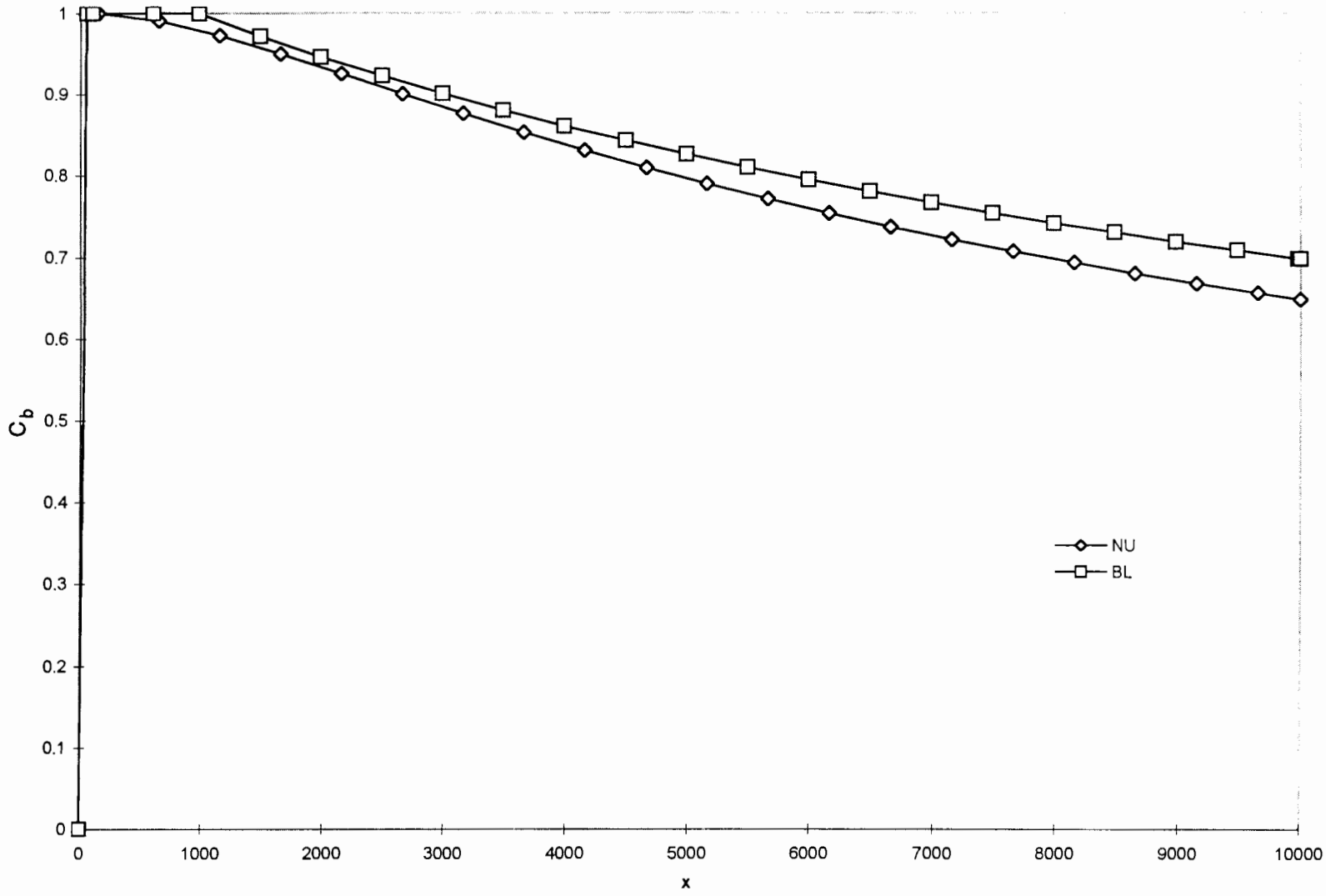

Figure 11c Comparison between values of C predicted by the TSBL method and rigorous numerical simulations ($q_R = 0.1$, $x_e = 100$)

(c) $a = 0.005$; $x_{max} = 10000$

Discussion

Presently there is a wide gap between our capability to apply sophisticated numerical models of transport phenomena in porous media and our ability to supply adequate input to such models. Such input must be based on the hard work of monitoring, sampling, laboratory studies, and field measurements. In order to reduce field efforts, it is possible to perform numerical simulations of sensitivity of the aquifer system to various parameters. In such a manner the set of parameters can be ranked in terms of importance and priority for determination. The TSBL method can be very helpful in determining parameter sensitivity and importance, and it may reduce the effort required to assess the basic characteristics of the domain of interest.

The present study has quantitatively described some possible mineralization scenarios associated with the seepage of saltwater into a freshwater aquifer, and has characterized the build-up of saltwater mounds. The simplified mathematical tools given in this study can be used for basic evaluation of field measurements. It is possible to get a rough estimate of the strength of the source of salinity (i.e. the rate of seepage of the saltwater multiplied by the extent of the impermeable layer discontinuity), and to predict possible characteristic values of dispersivities. Due to the simplicity of the TSBL method it is possible to apply simple regression curves and statistical analysis of field data, to provide good approximations of parameters characterizing the domain of interest. The analysis and presentation of the various regions subject to mineralization by use of comparatively simple definitions and terminology, which are applicable to any kind of calculation, can help visualize and compare the processes typical of inland aquifer mineralization.

The study refers to comparatively large values of q_R/a. In such a case, the saltwater mound may develop even for small values of x_e. However, it should be noted that even for comparatively small values of q_R/a, the saltwater mound might develop, provided that x_e is sufficiently large. We have simply referred to ranges of the dimensionless parameters, which seem to be reasonable for the Kansas examples. Generally, the saltwater mound develops according to the dimensionless ratio between the strength of the saltwater source and the dispersivity, i.e. the value of $x_e q_R/a$.

Summary and conclusions

This study applies a simplified conceptual model to mineralization of an inland aquifer. A freshwater aquifer is subject to mineralization due to the seepage of saltwater from deep formations saturated with saltwater through a discontinuity in an impermeable layer that generally separates the freshwater from the saltwater. In cases of high rates of seepage of the saltwater and small values of the transverse dispersivity, a saltwater mound can develop at the bottom of the aquifer. On top of the saltwater mound a transition zone consisting of an inner and outer BLs occurs. Expressions describing the salinity distribution in the mineralized domain are developed by use of the top specified boundary layer (TSBL) method. Simple analytical expressions concerning the development of the various types of BLs are also derived to describe the buildup of the saltwater mound.

Numerical simulations have indicated that the various categories of mineralized regions and BLs can be identified in an aquifer subject to mineralization. Similar salinity profiles can be found in the domain, provided that appropriate normalized salinity and coordinate values are used. Tests have identified appropriate values of the power coefficients that characterize salinity profiles in the mineralized domain.

The identification of similar salinity profiles permits the employment of a BL approach. This approach leads to use of the TSBL method, which provides good descriptions and estimates of important regions subject to mineralization. However, use of the TSBL method requires several approximations. Several calibration coefficients are identified and determined by evaluating numerical simulations. Their use improves the agreement between TSBL values and those produced by the numerical simulations.

This study indicates that the TSBL method can be a very useful, simple, and robust means for the initial characterization of cases in which saltwater mounds develop in an inland aquifer subject to mineralization. With little effort the results of this study can be useful for the interpretation of field measurements. The simple set of definitions and terminology associated with the TSBL approach can also be very useful in the visualization of the aquifer mineralization process.

ACKNOWLEDGMENTS

This work was supported under contracts between the Kansas Water Office and the Kansas Geological Survey. The authors are grateful for the assistance of Mark Schoneweis in preparing the illustrations.

Appendix A: BL development in the range of x-values: $0 \le x \le x_{0.5}$

We consider that in the outer BL the salinity profile is given by

$$C = C_b(1-\eta)^n; \quad \eta = \frac{y-\delta_b}{\delta_0-\delta_b} \tag{A1}$$

where n is a power coefficient found to be about 3.

It is considered that at $y = \delta_0$ the salinity practically vanishes. At $y = \delta$ the salinity is C_T. Figure 3 shows the salinity fluxes transferred between the various BLs.

By the employment of Leibniz's theorem and integration of the equation of salinity transport in the bottom and outer BLs we obtain

$$x = \frac{H(\tau)}{an(n+1)} \quad if \quad 0 \le x \le x_{0.5}, t \tag{A2}$$

$$t = \frac{H(\tau)}{an(n+1)} \quad if \quad t \le x \le x_{0.5} \tag{A3}$$

where

$$\tau = \delta_0 - \delta_b; \quad 0 \le \tau \le an/q_R \tag{A4}$$

$$H(\tau) = \frac{1}{2}\tau^2 + \frac{an}{q_R}\tau - \left(\frac{an}{q_R}\right)^2 \ln\left(1+\tau\frac{q_R}{an}\right) \tag{A5}$$

Here q_R is the ratio between the seeping saltwater specific discharge and the aquifer specific discharge.

At the upper limit value of τ given by eq. (A4), the expressions given by eqs. (A2) and (A5) yield

$$x_{0.5} = \frac{an}{q_R^2(n+1)}(1.5-\ln 2) \approx 0.8\frac{an}{q_R(n+1)} \tag{A6}$$

By further use of the expressions resulting from the integration of the equation of salinity transport in the bottom and outer boundary layers we obtain

$$C_b = \frac{\tau}{\tau + an/q_R} \tag{A7}$$

$$C_b\delta_b = \frac{q_R}{an(n+1)}\left[\frac{1}{2}\tau^2 + \left(\frac{an}{q_R}\right)^2 - \left(\frac{an}{q_R}\right)^3\left(\frac{1}{\tau + an/q_R}\right) - \left(\frac{an}{q_R}\right)^2 \ln\left(1+\tau\frac{q_R}{an}\right)\right] \tag{A8}$$

The region of interest (ROI) is defined as the region in which the value of C exceeds the defined acceptable value, C_T. Again using the integral expressions for the salinity transport we obtain

$$\eta_T = 1 - (C_T / C_b)^{1/n} \tag{A9}$$

where η_T is the value of η at the top of the ROI.

The ROI vanishes as long as the salinity is smaller than the acceptable value C_T. The build-up of the ROI occurs downstream of $x=x_b$. At x_b the value of C_b is equal to C_T. Rearrangements of variables yield

$$x_b = \frac{anC_T}{q_R^2(n+1)} \tag{A10}$$

$$(\delta)_{x=x_b} = (\delta_b)_{x=x_b} \approx \frac{anC_T}{2(n+1)q_R} \tag{A11}$$

Downstream of x_b the thickness of the ROI is given by

$$\delta = \delta_b + \tau - \tau^{1-1/n}\left[C_T(\tau + an/q_R)\right]^{1/n} \tag{A12}$$

Appendix B: BL development in the range of x-values $x_{0.5} \le x \le x_u$

According to Fig. 3, consideration of mass conservation in the inner BL and reference to eq. (20) yielded:

$$\frac{d}{dt}\left[\delta_u \frac{n_1 C_b + 0.5}{n_1 + 1}\right] = q_R - \frac{(C_b - 0.5)n_1}{\delta_u} \tag{B1}$$

In the outer BL we assumed the following salinity profile:

$$C = 0.5L(\eta); \quad \eta = \frac{y - \delta_u}{\delta_0 - \delta_u}; \quad \delta_u \le y \le \delta_0 \tag{B2}$$

The function L was represented by

$$L = (1 - \eta)^{n_2} \tag{B3}$$

According to Fig. 3, consideration of mass conservation in the outer BL and reference to eq. (B3) yielded:

$$\frac{d}{dt}(\delta_0 - \delta_u) = \frac{a n_2 (n_2 + 1)}{\delta_0 - \delta_u} \tag{B4}$$

Continuity of the salinity profile at $y = \delta_u$ yielded:

$$\frac{(C_b - 0.5)n_1}{\delta_u} = \frac{n_2}{\delta_0 - \delta_u} \tag{B5}$$

Rearrangement of terms yielded:

$$C_b = 0.5\left[1 + \left(\frac{n_2}{n_1}\right)\left(\frac{\delta_u}{\delta_0 - \delta_u}\right)\right] \tag{B6}$$

$$C_b = 0.5\left[1 + \frac{n_2}{n_1}\frac{\delta_u}{\delta_0 - \delta_u}\right] \tag{B6}$$

For comparatively large values of x the value of C_b approached unity, then

$$\frac{\delta_0}{\delta_u} \rightarrow \frac{n_1}{n_2} + 1 \tag{B7}$$

The build-up of the regions of inner and outer BLs started at $t = x_{0.5}$. The characteristics of these BLs were given by eqs. (20) and (B2). In following expressions values concerning $x < t$ are provided. For x-values larger than t, the parameter t should be inserted instead of x. In such a manner we avoided writing long expressions incorporating the step function.

Direct integration of eq. (B4) yielded:

$$(\delta_0 - \delta_u)^2 = 2an_2(n_2+1)(x - x_{0.5}) + (\delta_0 - \delta_u)^2_{x=x_{0.5}} \tag{B8}$$

It was convenient and very reasonable to assume

$$(\delta_0 - \delta_u)_{x=x_{0.5}} \approx (\delta_0 - \delta_b)_{x=x_{0.5}} \tag{B9}$$

$$(\delta_u)_{x=x_{0.5}} \approx (\delta_b)_{x=x_{0.5}} \tag{B10}$$

Only minor adjustment is usually needed to these expressions to comply with the conservation of mass principle.

We introduced eqs. (B5) and (B8) into eq. (B1) and performed a direct integration to obtain:

$$\begin{aligned}\delta_u\left(\frac{n_1 C_b + 0.5}{n_1 + 1}\right) = q_R(x - x_{0.5}) - \frac{1}{2(n_2+1)}\left[2an_2(n_2+1)(x - x_{0.5}) + (\delta_0 - \delta_u)^2_{x=x_{0.5}}\right]^{0.5} \\ + \frac{1}{2(n_2+1)}(\delta_0 - \delta_u)_{x=x_{0.5}} + \frac{1}{2}(\delta_u)_{x=x_{0.5}}\end{aligned} \tag{B11}$$

Introducing eq. (B6) into eq. (B11) we obtained:

$$\delta_u = \frac{(n_1+1)(\delta_0 - \delta_u)}{2n_2}\left[(1+F)^{0.5} - 1\right] \tag{B12}$$

where

$$F = \frac{8fn_2}{(n_1+1)(\delta_0 - \delta_u)} \tag{B13}$$

$$f = q_R(x - x_{0.5}) - \frac{1}{2(n_2+1)}\left[(\delta_0 - \delta_u) - (\delta_0 - \delta_u)_{x=x_{0.5}}\right] + \frac{1}{2}(\delta_u)_{x=x_{0.5}} \quad \text{(B14)}$$

The top of the ROI was again defined by the isohaline $C = C_T$. Applying eq. (B2) we obtained:

$$\eta_T = 1 - (2C_T)^{1/n_2} \quad \text{(B15)}$$

$$\delta = \delta_u + (\delta_0 - \delta_u)\eta_T = \delta_u\eta_T + (1 - \eta_T)\delta_u \quad \text{(B16)}$$

Appendix C: BL development in the range of x-values $x_u \leq x \leq x_e$

Fluxes of salinity transferred between the various BL are shown in Fig. 3. According to this figure no flux of salinity is transferred from the completely saline bottom BL into the inner BL. It is approximated that the inner and outer BL develop around a floating boundary represented by the isohaline $C = 0.5$. However, the location of this isohaline depends very much on the rate of seepage of the saltwater into the aquifer. Therefore, as shown hereafter, we determine the development of the bottom saltwater BL by applying the conservation of mass principle with regard to the complete region subject to mineralization.

According to Fig. 3, as well as an integration of the salinity transport, consideration of mass conservation in the inner BL and eq. (35) yields

$$\frac{d}{dt}\left[(\delta_u - \delta_b)^2\left(\frac{n_3 + 0.5}{n_3 + 1}\right)\right] = an_3 \tag{C1}$$

Direct integration of eq. (C1) yields

$$(\delta_u - \delta_b)^2 = \alpha_1 a \frac{n_3(n_3 + 1)}{n_3 + 0.5}(x - x_u) + (\delta_u^2)_{x=x_u} \tag{C2}$$

This expression is useful if $t>x$. Otherwise t should replace x in this equation.

The coefficient α_1 in eq. (C2) is a calibration coefficient. Its determination is discussed and evaluated in the "calibration section".

With regard to the outer BL, we again integrate the equation of salinity transport to obtain

$$\frac{d}{dt}(\delta_0 - \delta_u)^2 = 2an_4(n_4 + 1) \tag{C3}$$

Direct integration of this expression and introduction of a calibration coefficient α_2 yield:

$$(\delta_0 - \delta_u)^2 = 2\alpha_2 a n_4 (n_4 + 1)(x - x_u) + (\delta_0 - \delta_u)^2_{x=x_u} \tag{C4}$$

Again, this expression is useful if $t>x$. Otherwise t should replace x in this equation. The coefficient α_2 is also a calibration coefficient.

The identity of the salinity gradient at both sides of the isohaline $C = 0.5$ yields

$$\frac{n_4}{n_3} = \frac{\delta_0 - \delta_u}{\delta_u - \delta_b} \tag{C5}$$

Applying the principle of mass conservation for the whole region of the salinity intrusion, we obtain

$$\delta_b = \alpha_3 q_R (x - x_u) - \frac{1}{2(n_4 + 1)}\left[(\delta_0 - \delta_u) - (\delta_0 - \delta_u)_{x=x_u}\right]$$

$$- \frac{n_3 + 0.5}{n_3 + 1}\left[(\delta_u - \delta_b) - (\delta_u)_{x=x_u}\right] \tag{C6}$$

Here also we introduce a calibration coefficient α_3.

Equation (C6) provides the expression describing the development of the saltwater mound in the domain.

With regard to the determination of the ROI, it should be noted that eqs (31) and (32) are also applicable to this range of x-values.

Appendix D: BL development in the range of x-values $x \geq x_1$

Continuity of the slope of the salinity profile at $y = \delta_u$ required:

$$\frac{\delta_0}{\delta_u} = \frac{c_r n_6}{(1-c_r)n_5} \tag{D1}$$

Conservation of mass implied for the inner BL

$$\frac{\partial}{\partial t}\left(\int_0^{\delta_u} C dy\right) + \frac{\partial}{\partial x}\left(\int_0^{\delta_u} C dy\right) = 0 \tag{D2}$$

Referring to a moving coordinate system we obtained:

$$\frac{d}{dt}(C_b \delta_u) = 0 \tag{D3}$$

Therefore

$$(C_b \delta_u)_x = (C_b \delta_u)_{x_1} \tag{D4}$$

We considered that the vertical salinity gradient did not lead to salinity transport between the inner and outer BLs, but led to the expansion of the two BLs. Therefore, we obtained for the inner BL

$$C_{avu} \frac{d\delta_u}{dt} = -\alpha_5 a \left(\frac{\partial C}{\partial y}\right)_{y=\delta_u} \tag{D5}$$

where α_5 is a coefficient; C_{avu} is the average salinity of the inner BL

$$C_{avu} = \frac{1}{\delta_u}\int_0^{\delta_u} C dy \tag{D6}$$

Introducing the appropriate value of C_{avu} into eq. (D5) we obtained

$$\frac{d\delta_u}{dt} = \alpha_5 \frac{2a(1-c_r)n_5(n_5+1)}{n_1 + c_r} \tag{D7}$$

Direct integration of this expression yielded

$$(\delta_u)_x = (\delta_u)_{x_1} + \alpha_5 \frac{2a(1-c_r)n_5(n_5+1)}{n_5+c_r}(x-x_1) \tag{D8}$$

It should be noted that eqs. (D4) and (D8) refer to steady state conditions, in which values of BL thickness are kept constant.

Principles of contaminant transport were also used with regard to the outer BL.

We again considered that salinity gradients in the outer BL led to its expansion and obtained

$$C_{avo}\frac{d}{dt}(\delta_0-\delta_u) = -\alpha_6 a\left(\frac{\partial C}{\partial y}\right)_{y=\delta_u} \tag{D9}$$

where α_6 is a coefficient; C_{avo} is the average salt concentration in the outer BL.

$$C_{avo} = \frac{1}{\delta_0-\delta_u}\int_{\delta_u}^{\delta_0} C dy \tag{D10}$$

Introducing eq. (42) into eq. (D10) we obtained:

$$C_{avo} = C_b\frac{c_r}{n_6+1} \tag{D11}$$

Introducing eqs. (42) and (D11) into eq. (D10) we obtained:

$$\frac{d}{dt}(\delta_0-\delta_u)^2 = 2\alpha_6 a n_6(n_6+1) \tag{D12}$$

Direct integration of this expression and reference to the boundary conditions at $x = x_1$ yielded:

$$(\delta_0-\delta_u)_x^2 = (\delta_0-\delta_u)_{x_1}^2 + 2\alpha_6 a n_6(n_6+1)(x-x_1) \tag{D13}$$

Appendix E: Adjustment of BL thickness values at interfaces between adjacent ranges of x-values

Figures 2 and 3, as well as the relevant equations indicate that in different ranges of x-values different power laws represent the salinity distribution. Therefore, compliance with the principle of mass conservation requires some adjustment of the BL thickness values at the interfaces between adjacent ranges of x-values. In the following paragraphs such adjustments are presented.

Adjustment at $x_{0.5}$

Conservation of mass of salinity on both sides of the aquifer cross section represented by $x_{0.5}$ lead to the following relationship:

$$\left\{\delta_b C_b + C_b \frac{\delta_0 - \delta_b}{n+1}\right\}_{left} = \left\{0.5 C_b \frac{\delta_0 - \delta_u}{n_2 + 1} + \delta_u \frac{C_b(n_1 + 2) - 0.5}{n_1 + 1}\right\}_{right} \qquad \text{(E1)}$$

where subscripts *left* and *right* refer to the upstream and downstream sides of $x_{0.5}$, respectively, which are represented in Figs. 2 and 3, as the left and right hand sides of this point.

Equation (E1) was obtained by integrating the salinity profile over the aquifer thickness, namely between the bottom of the aquifer and $y = \delta_0$ at both sides of $x_{0.5}$.

Equation (E1) incorporates three unknown quantities at the right side of $x_{0.5}$, namely C_b, δ_u and δ_0. Numerical experiments indicated that it was appropriate to consider that the value of δ_0 was identical on both sides of $x_{0.5}$. The value of this parameter is not crucial for the calculation of salinity distribution in the simulated domain. It approximates the location of very small salinity value. Therefore, eq. (E1) indicates that some adjustment to values of C_b and δ_u is needed. However, this equation still leaves some freedom with regard to the appropriate adjustment of each one of this parameters. Several options were tested: 1) identity of the value of δ_b on the left hand side to the value of δ_u on the right hand side of $x_{0.5}$, and 2) identity of the salinity flux conveyed through the

bottom BL on the left side of $x_{0.5}$ to the salinity flux conveyed through the inner BL on the right hand side of $x_{0.5}$. Comparison of BL simulations to numerical results indicated that the first option was simpler to implement and provided good agreement with the numerical simulation results.

Adjustment at x_u and x_e

We integrate the salinity profile over the mineralized zone at both sides of the point x_u. Then, according to the principle of mass conservation, we obtain:

$$\left\{0.5\frac{\delta_0-\delta_u}{n_2+1}+\delta_u\frac{(n_1+2)-0.5}{n_1+1}\right\}_{left}=\left\{0.5\frac{\delta_0-\delta_u}{n_4+1}+\delta_u\frac{(n_1+2)-0.5}{n_3+1}\right\}_{right} \quad \text{(E2)}$$

By assuming that the value of δ_0 is identical at both sides of x_u eq. (E2) is used to determine the value of δ_u at the right hand side of x_u.

As there is no change in values of power coefficients at x_e, there is no need for adjustment of the values of BL thickness at that point.

Adjustment at x_1

We integrate the salinity profile over the mineralized zone at both sides of sides of point x_1. Then according to the principle of mass conservation, we obtain:

$$\left\{0.5\frac{\delta_0-\delta_u}{n_4+1}+\delta_u\frac{(n_3+2)-0.5}{n_3+1}\right\}_{left} =\left\{0.5C_b\frac{\delta_0-\delta_u}{n_6+1}+\delta_u\frac{C_b(n_5+2)-0.5}{n_5+1}\right\}_{right} \quad \text{(E3)}$$

Equation (E3) incorporates 3 unknown quantities on the right hand side of point x_1: C_b, δ_u, and δ_0. It was found appropriate to assume that the value of δ_0 is identical at both sides of x_1. It was also found appropriate to assume that the salinity flux from the left inner BL is conveyed into the right inner BL. It should be noted that such an assumption

implies that also the salinity flux of the left outer BL is conveyed into the right outer BL. This assumption provides a second equation:

$$\left\{\delta_u \frac{(n_3+2)-0.5}{n_3+1}\right\}_{left} = \left\{\delta_u \frac{C_b(n_5+2)-0.5}{n_5+1}\right\}_{right} \qquad \text{(E4)}$$

Equations (E3) and (E4) can be used to calculate values of C_b and δ_u at the right hand side of x_1.

Numerical simulations indicated that the values of the power coefficients n_5 and n_6 should be modified downstream of x_1 at a distance of about 10 times the extent of the saltwater mound. When such a measure is taken some adjustment of C_b and δ_u values should be made.

Notation

a dimensionless transverse dispersivity

a_L dimensionless longitudinal dispersivity

BL boundary layer; value obtained by boundary layer approximation

c_r ratio between the salinity at $y=\delta_u$ and C_b

C normalized salt concentration (salinity)

C_b normalized salinity at the bottom of the ROI

C_T normalized salinity at the top of the ROI

C^* salt concentration (salinity) [ML^{-3}]

C_f^* salinity of freshwater [ML^{-3}]

C_s^* salinity of saltwater [ML^{-3}]

$\tilde{D}$ dispersion tensor [L^2T^{-1}]

D_x longitudinal dispersion coefficient [L^2T^{-1}]

D_y transverse dispersion coefficient [L^2T^{-1}]

f function defined in eq. (30)

F function defined in eq. (29)

g gravitational acceleration [LT^{-2}]

H a function of τ defined by eq. (22)

k permeability [L^2]

l_0 length scale [L]

n, n_i $(i = 1,..,6)$ power coefficients

NU value obtained by numerical simulation

p pressure [$ML^{-1}T^{-2}$]

q specific discharge [LT^{-1}]

q_R ratio between the specific discharges of the seeping saltwater and the aquifer

ROI region of interest - the top specified boundary layer (TSBL)

t dimensionless time

t_e dimensionless time needed to advect fluid particle from x_e to x

t^* time [T]

TSBL top specified boundary layer

V interstitial flow velocity [LT^{-1}]

x dimensionless longitudinal coordinate

x_b starting point for the development of the ROI

$x_{0.5}$ point at the bottom boundary where $C_b = 0.5$

x_1 point at the bottom boundary where $x > x_e$, and C_b becomes smaller than 1

x_e dimensionless length of the impermeable layer discontinuity

x_{max} dimensionless horizontal extent of the domain

x_u point at the bottom boundary where $x < x_e$, and $C_b = 1$

x^* longitudinal coordinate [L]

x_e^* length of the impermeable layer discontinuity [L]

y dimensionless vertical coordinate

y^* vertical coordinate [L]

α_i $(i = 1,..,6)$ calibration coefficients

δ dimensionless thickness of the ROI

δ_0 dimensionless ordinate of practically vanishing salinity

δ_b dimensionless thickness of the bottom boundary layer or saltwater mound

δ_R ratio between the thickness of the outer and inner boundary layers

δ_u dimensionless ordinate associated with $C/C_b = 0.5$.

ζ modified vertical coordinate

η dimensionless coordinate of the outer BL

η_T value of η at $y = \delta$

μ fluid viscosity [$ML^{-1}T^{-1}$]

ρ fluid density [ML^{-3}]

τ dimensionless thickness of the outer BL

ξ coordinate of the inner BL

ξ_T value of ξ at $y=\delta$

References

Allen, J.R.L., 1974. Studies in fluviatile sedimentation - implications of pedogenic carbonate units, Lower Old Red Sandstone, Anglo-Welsh Outcrop. Geology Journal, 9: 181-208

Allen, P.A., and Collinson, J.D., 1986. Lakes, in "Sedimentary Environments and Facies", H.G. Reading (ed.), 2nd Edition pp. 63-94, Blackwell Scientific Pub., Oxford, England.

Bayne, C.K., and O'Connor, H.G., 1968. Quaternary system, in "The Stratigraphic Succession in Kansas", D.E. Zeller (ed.), Bulletin 189, pp. 59-67, Kansas Geological Survey, The University of Kansas, Lawrence, Kansas.

Boellstroff, J., 1976. The succession of late Cenozoic volcanic ashes in the Great Plains - aprogress report , in "Stratigraphy and faunal sequences - Meade Co., Guidebook Series 1, pp. 37-38, Kansas Geological Survey, The University of Kansas, Lawrence, Kansas.

Buddemeier, R.W., Garneau, G.W., Healey, J.M., Ma T.-S., Sophocleous, M.A., Wittemore, D.O., Young, D.P., and Zehr, D., 1993. The mineral intrusion project - report of progress during fiscal year 1993, Open-file Report 93-23, Kansas Geological Survey, The University of Kansas, Lawrence, Kansas.

Buddemeier, R.W., Falk, S., Garneau, G.W., Laterman, J., Ma, T.-S., Sophocleous, M.A., Whittemore, D.O., Young, D.P., and Zehr, D., 1994. The mineral intrusion project: investigation of salt contamination of ground water in the eastern Great Bend Prairie aquifer - progress and activities during fiscal year 1994, Open-file Report 94-28, Kansas Geological Survey, The University of Kansas, Lawrence, Kansas.

Collinson, J.D., 1986. Alluvial sediments, in "Sedimentary Environments and Facies", H.R. Reading (ed.),2nd Edition, pp. 20-62, Blackwell Scientific Pub., Oxford, England.

Fader, S.W., and Stullken, L.E., 1978. Geohydrology of the Great Bend Prairie - south-central Kansas, Irrigation series 4, Kansas Geological Survey, The University of Kansas, Lawrence, Kansas.

Garneau, G.W., 1995. Detection and characterization of the distribution of mineral intrusion in the Great Bend Prairie aquifer - south-central Kansas, Open-file Report 95-35, Kansas Geological Survey, The University of Kansas, Lawrence, Kansas.

Gillespie, J.B., and Hargadine, G.D., 1994. Geohydrology and saline groundwater discharge to the South Fork Ninnescah River in Pratt and Kingman Counties, Water Resources Investigation Report 93-4177, U.S. Geological Survey.

Hallman, A., 1981. Facies interpretation and the stratigraphic record, W.H. Freeman and Co., San Francisco, California.

Layton, D.W., and Berry, D.W., 1973. Geology and groundwater resources Pratt County south-central Kansas, Bulletin 205, Kansas Geological Survey, The University of Kansas, Lawrence, Kansas.

Rubin, H., and Buddemeier, R.W., 1996. A top specified boundary layer (TSBL) approximation approach for the simulation of groundwater contamination processes, accepted for publication in J. of Contaminant Hydrology, 22: 123 – 144.

Rubin, H., and Buddemeier, R.W., 1998a. Application of the top specified boundary layer (TSBL) approximation to initial characterization of an inland aquifer mineralization-Part 1: Direct contact between fresh and saltwater, Journal of Contaminant Hydrology, 32/3-4: 149-172.

Rubin, H., and Buddemeier, R.W., 1998b. Application of the top specified boundary layer (TSBL) approximation to initial characterization of an inland aquifer mineralization-Part 2: Seepage of saltwater through semi-confining layers, Journal of Contaminant Hydrology, 32/3-4: 173-198.

Rubin, H., and Buddemeier, R.W., 1998c. Approximate analysis of groundwater mineralization due to local discontinuities in impermeable layer - Part 1 Direct contact

between fresh and saltwater, Open-File Rept. No. 98-31, Kansas Geological Survey, The University of Kansas, Lawrence, Kansas.

Rubin, H., and Buddemeier, R.W., 1998d. Approximate analysis groundwater mineralization due to local discontinuities in impermeable layer - Part 2: Seepage of saltwater through semi-confining discontinuity, Open-File Rept. No. 98-32, Kansas Geological Survey, The University of Kansas, Lawrence, Kansas.

Stullken, L.E., and Fader, S.W., 1976. Hydrogeologic data from the Great Bend Prairie - south-central Kansas, Ground-water Release No. 5, Kansas Geological Survey, The University of Kansas, Lawrence, Kansas.

Ward, P.A., Carter, B.J., and Weaver, B., 1993. Volcanic ashes - time markers in soil parent materials of the southern plains, Soil Science Society Journal, 57: 453-460.

Welch, J.E., and Hale, J.M., 1987. Pleistocene loess in Kansas - status, present problems and future considerations, Guidebook Series 5, pp. 67-84, Kansas Geological Survey, The University of Kansas, Lawrence, Kansas.